DFT for Nuclear Physics

Thomas Papenbrock

and OAK RIDGE NATIONAL LABORATORY

UNEDF SciDAC Collaboration
Universal Nuclear Energy Density Functional

SciDAC
Scientific Discovery through Advanced Computing

NUCLEI
Nuclear Computational Low-Energy Initiative

EMMI workshop *From Ultracold Fermi Gases to Neutron-rich Many-Body Systems: Universal Aspects and Modern Approaches to Density Functional Theory*
Darmstadt, March 18-22 2013

Research partly funded by the US Department of Energy

Universal Nuclear Energy Density Functional

http://unedf.org/

- 15 institutions
- ~50 researchers
  - physics
  - computer science
  - applied mathematics
- foreign collaborators
- annual budget $3M
- 2008-2012

Bottom-up approach to nuclear structure

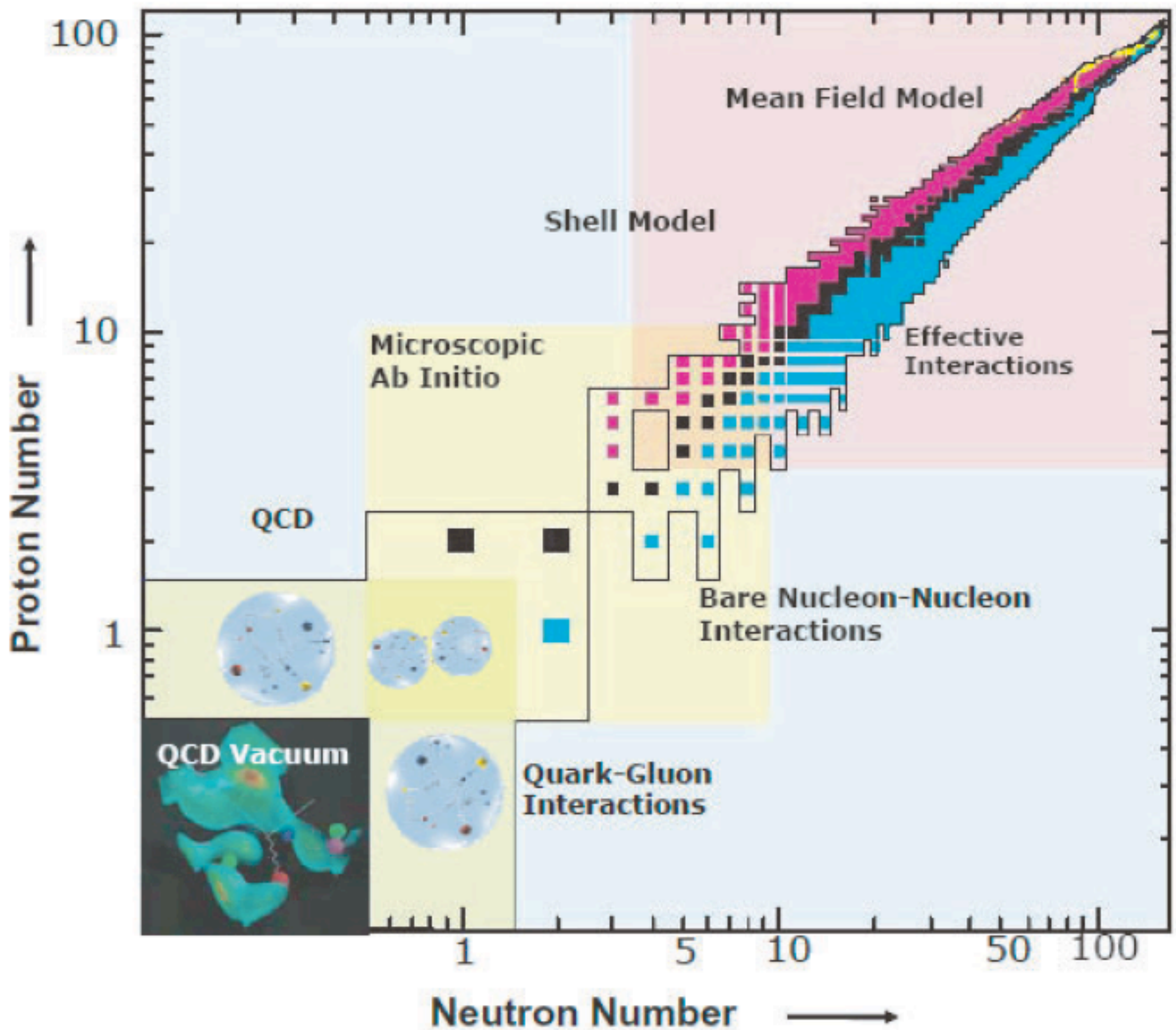

Figure from A. Richter (2004)

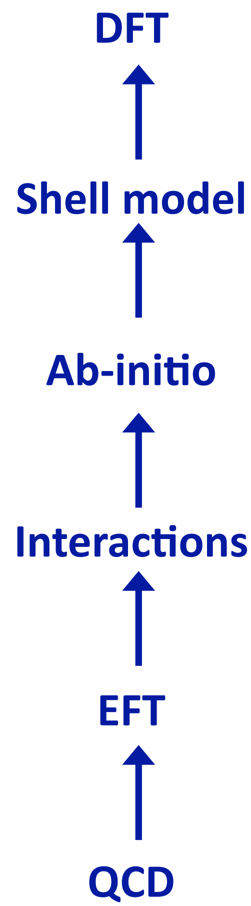

Methods across the nuclear chart

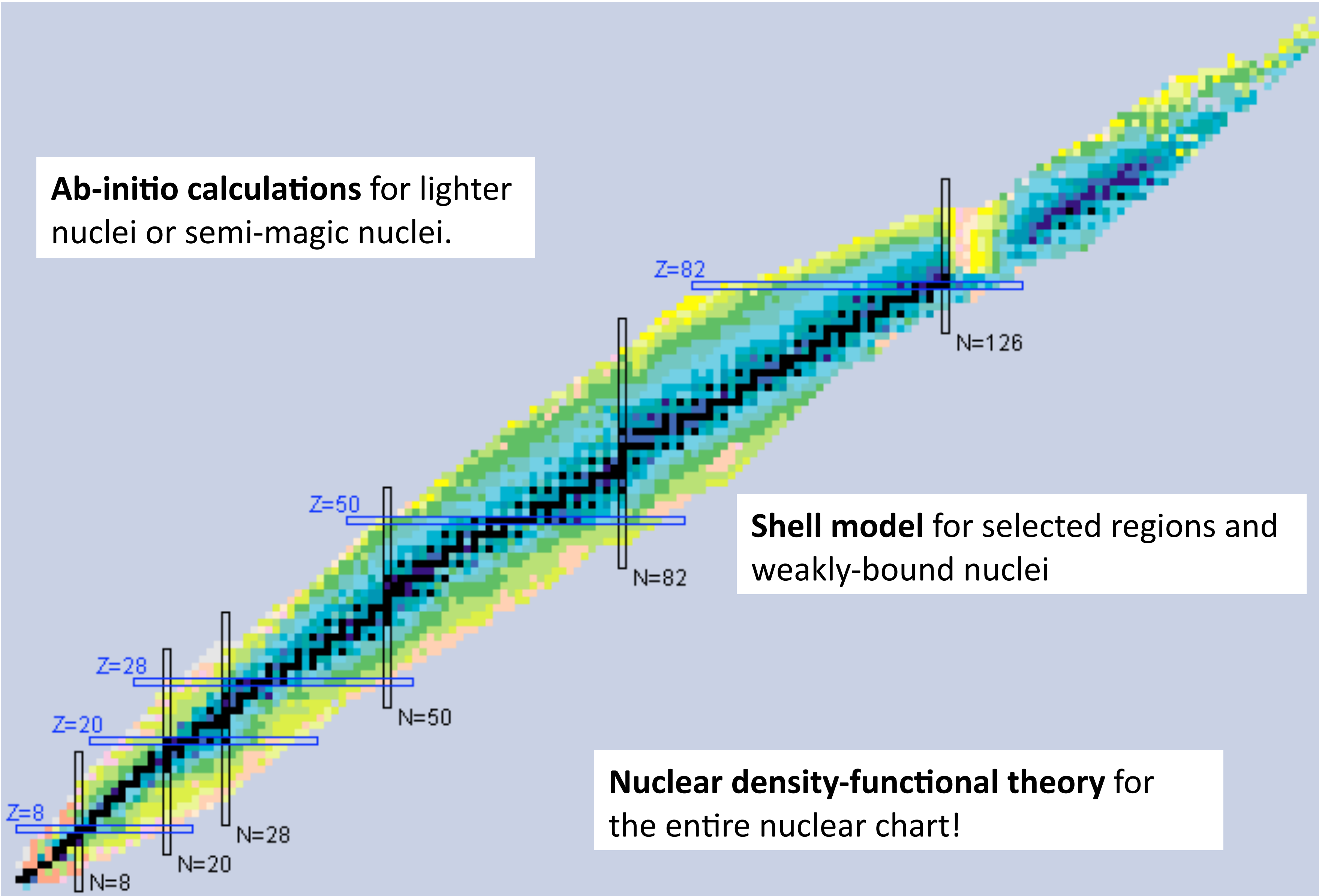

Ab-initio calculations for lighter nuclei or semi-magic nuclei.

Shell model for selected regions and weakly-bound nuclei

Nuclear density-functional theory for the entire nuclear chart!

UNEDF0 functional

Kortelainen, Lesinski, Moré, Nazarewicz, Sarich, Schunck, Stoitsov, Wild, Phys. Rev. C 82, 024313 (2010)

- Energy functional based on Skyrme SLy4 parametrization

$$E = \int \mathcal{H}(\boldsymbol{r}) d^3\boldsymbol{r}$$

- usual kinetic part (with 1/A mass shift); interaction: $\chi = \chi_0 + \chi_1$
- interaction energy functional (with isospin labels): 13 parameters

$$\begin{aligned}\chi_t(\boldsymbol{r}) \;&=\; C_t^{\rho\rho}\rho_t^2 + C_t^{\rho\tau}\rho_t\tau_t + C_t^{J^2}\boldsymbol{J}_t^2 \\ &\quad + C_t^{\rho\Delta\rho}\rho_t\Delta\rho_t \; + C_t^{\rho\nabla J}\rho_t\boldsymbol{\nabla}\cdot\boldsymbol{J}_t \\ C_t^{\rho\rho} &= C_{t0}^{\rho\rho} + C_{t\mathrm{D}}^{\rho\rho}\;\rho_0^\gamma\end{aligned}$$

- Pairing part depends on local pairing density: 2 parameters

$$\breve{\chi}(\boldsymbol{r}) = \sum_{q=n,p} \frac{V_0^q}{2}\left[1 - \frac{1}{2}\frac{\rho(\boldsymbol{r})}{\rho_0}\right]\breve{\rho}^2(\boldsymbol{r})$$

UNEDF0 functional

Several parameters constrained from nuclear matter properties

$\{C^{\rho\rho}_{t0}, C^{\rho\rho}_{t\mathrm{D}}, C^{\rho\Delta\rho}_{t}, C^{\rho\tau}_{t}, C^{J^2}_{t}, C^{\rho\nabla J}_{t}\}_{t=0,1}$ and γ

- Equation of state (EOS) of symmetric nuclear matter around saturation

$$W(\rho_0) = \left(\frac{\hbar^2}{2m} + C^{\rho\tau}_0 \rho_0\right) C_{\mathrm{k}} \rho_0^{2/3} + \left(C^{\rho\rho}_{00} + C^{\rho\rho}_{0D}\rho_0^{\gamma}\right)\rho_0. \qquad \rho_0 = 0.16\,\mathrm{fm}^{-3}$$

- EOS of asymmetric nuclear matter

$$W(I,\rho_0) = \left(\frac{\hbar^2}{2m} + C^{\rho\tau}_0 \rho\right) C_{\mathrm{k}}\, \rho_0^{2/3}\, F_{+}(I) + C^{\rho\tau}_1 C_{\mathrm{k}}\, \rho_0^{5/3}\, I F_{-}(I) + \left[C^{\rho\rho}_{00} + C^{\rho\rho}_{0D}\rho_0^{\gamma} + I^2\left(C^{\rho\rho}_{10} + C^{\rho\rho}_{1D}\rho_0^{\gamma}\right)\right]\rho_0$$

$$F_{\pm}(I) = \frac{1}{2}\left[(1+I)^{5/3} \pm (1-I)^{5/3}\right]$$

- Parameters $\{\rho_{\mathrm{c}}, E^{\mathrm{NM}}/A, M^*_s, K^{\mathrm{NM}}, a^{\mathrm{NM}}_{\mathrm{sym}}, L^{\mathrm{NM}}_{\mathrm{sym}}, M^*_v, C^{\rho\Delta\rho}_0, C^{\rho\Delta\rho}_1, C^{\rho\nabla J}_0, C^{\rho\nabla J}_1, C^{J^2}_0, C^{J^2}_1\}$

UNEDF0 functional

- Pairing parameters from odd-even staggering (OES); Lipkin-Nagomi for particle number projections
- Optimization employs POUNDerS [Practical Optimization Using No Derivatives (of Squares)]
- (pseudo) observables: nuclear matter properties, binding energies, radii, OES of 44 well-deformed even-even nuclei and 28 spherical nuclei

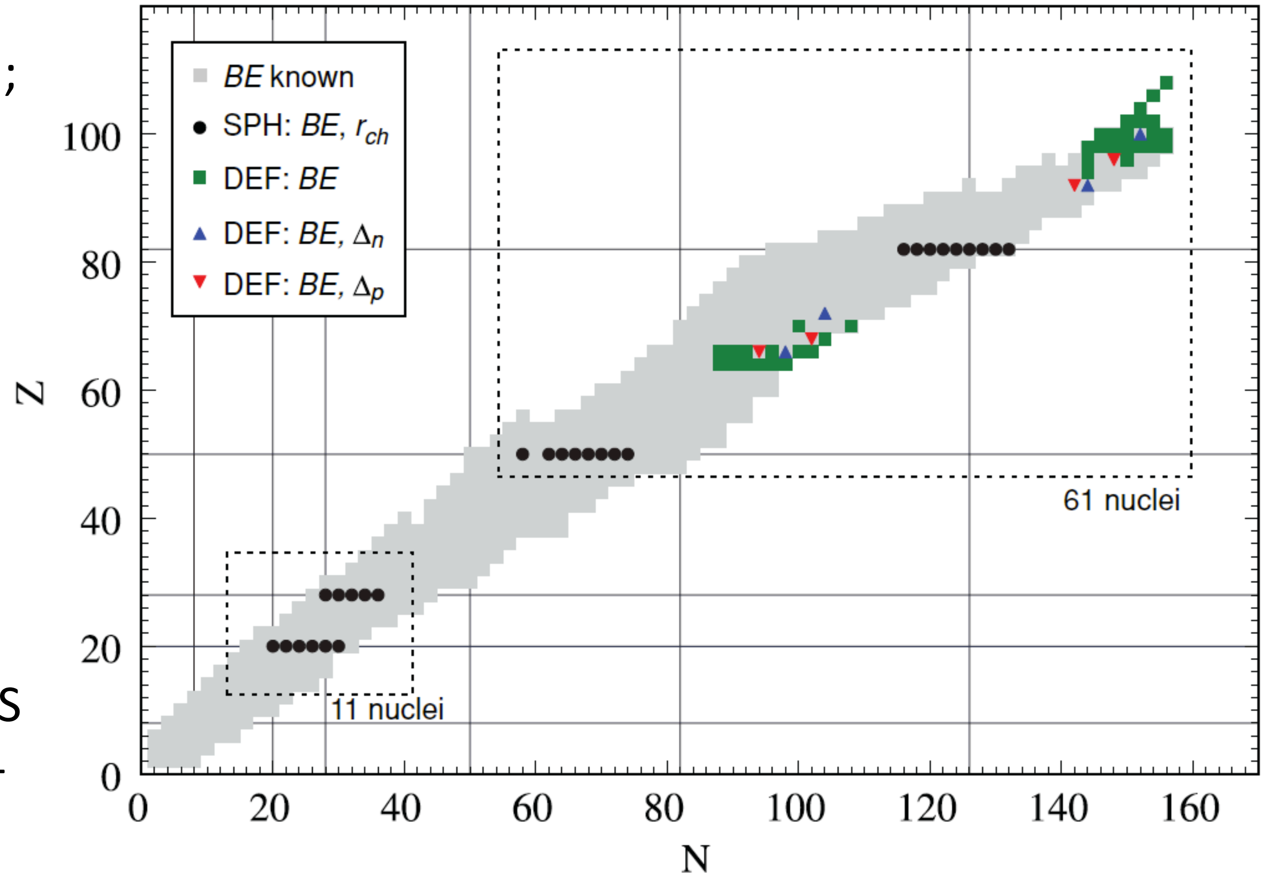

FIG. 1. (Color online) Experimental set of fit observables used in this work. The set contains data for 11 nuclei with $A < 66$ and 61 nuclei with $A > 106$.

Kortelainen, Lesinski, Moré, Nazarewicz, Sarich, Schunck, Stoitsov, Wild, Phys. Rev. C 82, 024313 (2010)

Optimization of UNEDF0 via POUNDerS

POUNDerS

• builds a quadratic model and does not require derivatives.

• fairly robust against noise

• finds acceptable minima

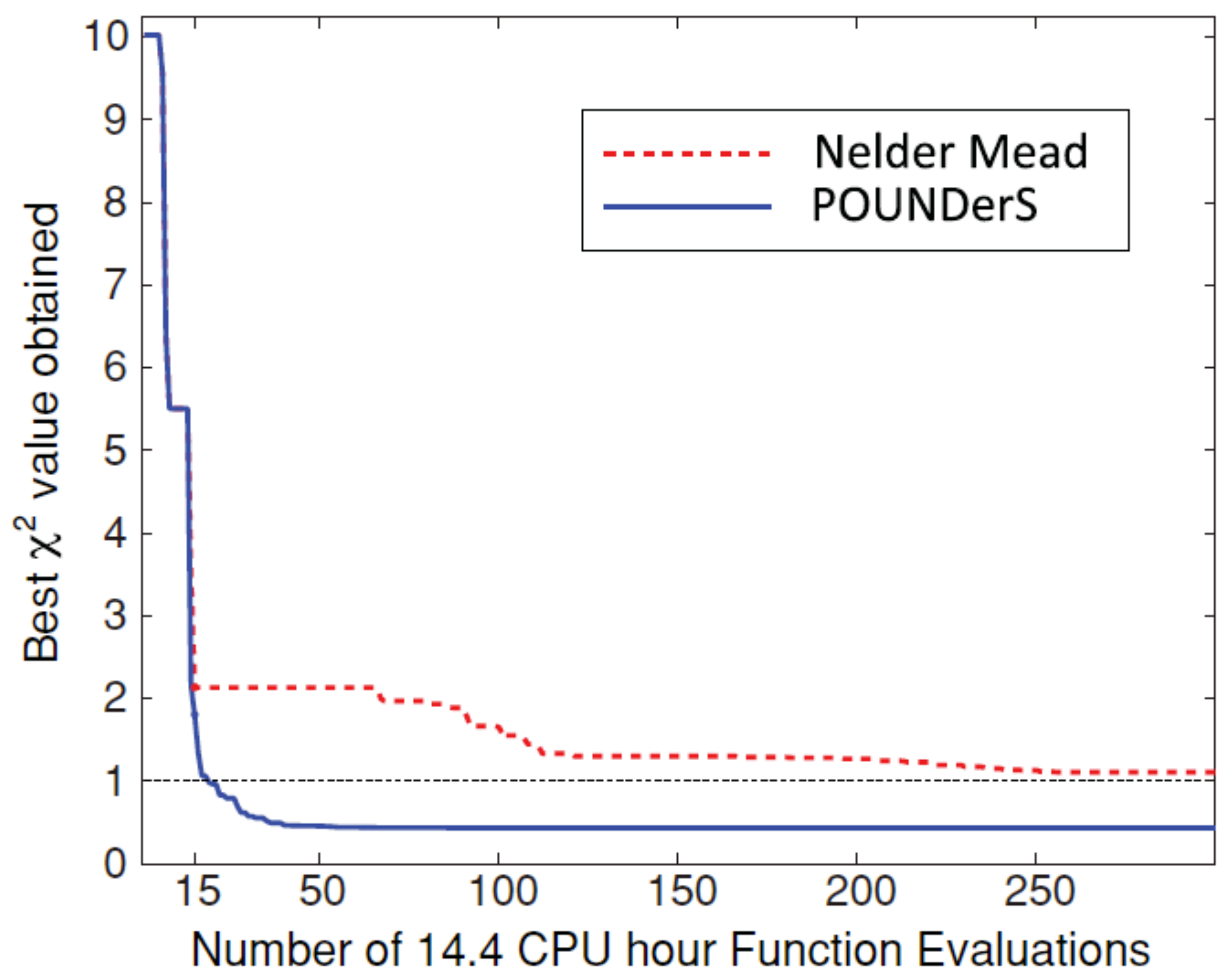

POUNDerS = **P**ractical **O**ptimization **U**sing **N**o **Der**ivatives (for **S**quares)
[J. Moré and S. Wild (2009)]

Optimized parameters

unedfnb (no bounds) χ^2 = 1.65 MeV on masses

k	$\mathbf{x}$	Scaling Interval *	$\hat{\mathbf{x}}^{(\mathrm{init.})}$	$\hat{\mathbf{x}}^{(\mathrm{fin.})}$
1.	ρ_c	[+0.14 , +0.18]	+0.160	0.151046
2.	E^{NM}/A	[-17.00, -15.00]	-15.972	-16.0632
3.	K^{NM}	[+170.00, +270.00]	+229.901	337.878
4.	$a_{\mathrm{sym}}^{\mathrm{NM}}$	[+27.00, +37.00]	+32.004	32.455
5.	$L_{\mathrm{sym}}^{\mathrm{NM}}$	[+30.00, +70.00]	+45.962	70.2185
6.	$1/M_s^*$	[+0.80, +2.00]	+1.439	0.95728
7.	$C_0^{\rho\Delta\rho}$	[-100.00, -40.00]	-76.996	-49.5135
8.	$C_1^{\rho\Delta\rho}$	[-100.00, +100.00]	+15.657	33.5289
9.	V_0^n	[-350.00, -150.00]	-258.200	-176.796
10.	V_0^p	[-350.00, -150.00]	-258.200	-203.255
11.	$C_0^{\rho\nabla J}$	[-120.00, -50.00]	-92.250	-78.4564
12.	$C_1^{\rho\nabla J}$	[-100.00, +50.00]	-30.750	63.9931

* Required by POUNDerS

Optimized parameters

unedf0 (hard bounds from nuclear matter properties) χ^2 = 1.45 MeV on masses

k	$\mathbf{x}$	Bounds	$\hat{\mathbf{x}}^{(\mathrm{init.})}$	$\hat{\mathbf{x}}^{(\mathrm{fin.})}$
1.	ρ_c	[+0.15,+0.17]	+0.160	0.160526
2.	E^{NM}/A	[-16.2,-15.8]	-15.972	-16.0559
3.	K^{NM}	[+190, +230]	+229.901	230
4.	$a_{\mathrm{sym}}^{\mathrm{NM}}$	[+28, +36]	+32.004	30.5429
5.	$L_{\mathrm{sym}}^{\mathrm{NM}}$	[+40, +100]	+45.962	45.0804
6.	$1/M_s^*$	[+0.9, +1.5]	+1.439	0.9
7.	$C_0^{\rho\Delta\rho}$	$[-\infty, +\infty]$	-76.996	-55.2606
8.	$C_1^{\rho\Delta\rho}$	$[-\infty, +\infty]$	+15.657	-55.6226
9.	V_0^n	$[-\infty, +\infty]$	-258.200	-170.374
10.	V_0^p	$[-\infty, +\infty]$	-258.200	-199.202
11.	$C_0^{\rho\nabla J}$	$[-\infty, +\infty]$	-92.250	-79.5308
12.	$C_1^{\rho\nabla J}$	$[-\infty, +\infty]$	-30.750	45.6302

Some results of the optimization of UNEDF0

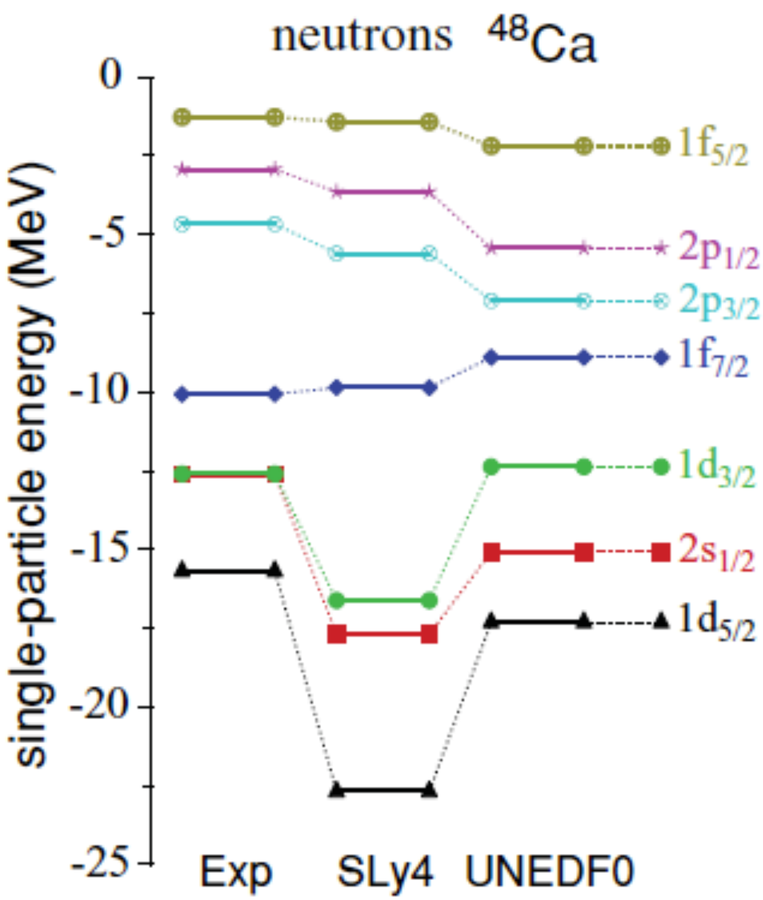

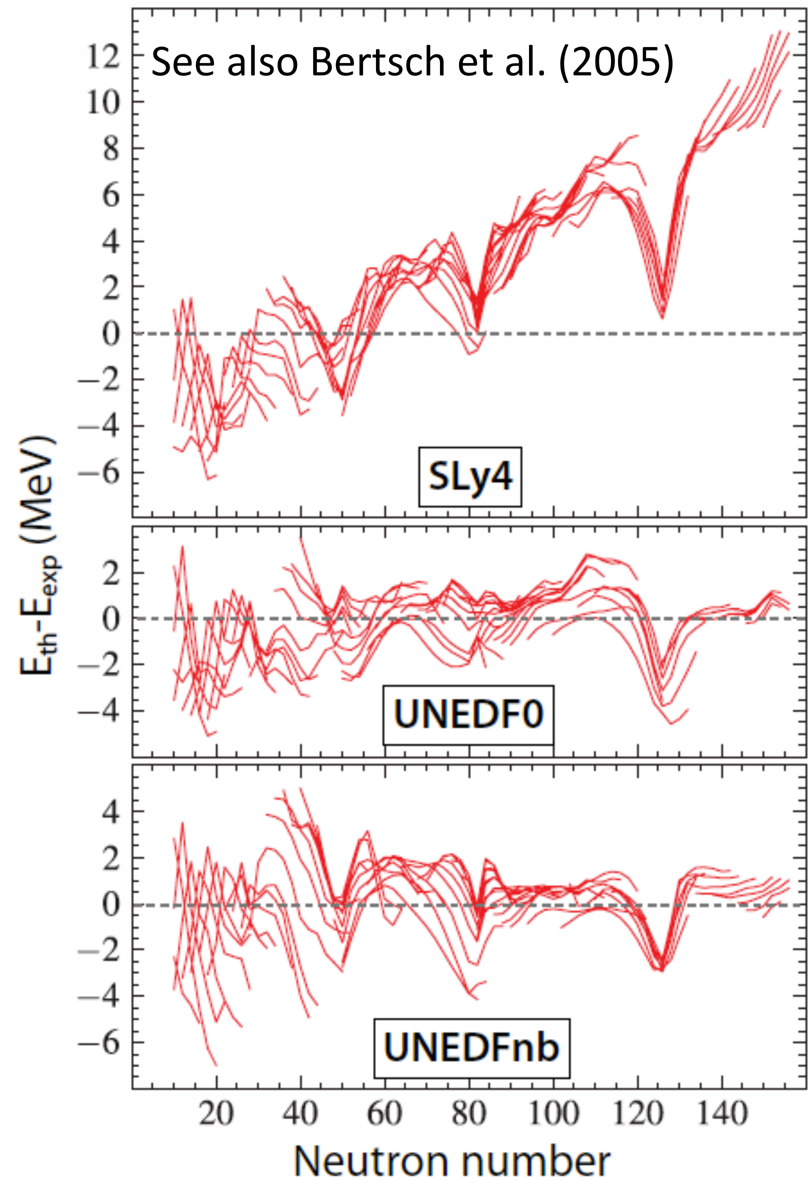

Correlation matrix [unedf0]

ρ_c	1.00											
E^{NM}/A	-0.28	1.00										
K^{NM}	–	–	–									
$a_{\mathrm{sym}}^{\mathrm{NM}}$	-0.10	-0.88	–	1.00								
$L_{\mathrm{sym}}^{\mathrm{NM}}$	-0.17	-0.80	–	$\boxed{0.97}$	1.00							
$1/M_s^*$	–	–	–		–	–						
$C_0^{\rho\Delta\rho}$	0.09	0.80	–	-0.81	-0.74	–	1.00					
$C_1^{\rho\Delta\rho}$	0.20	0.35	–	-0.47	-0.66	–	0.23	1.00				
V_0^n	0.02	0.21	–	-0.23	-0.25	–	0.23	0.23	1.00			
V_0^p	-0.13	-0.42	–	0.52	0.56	–	-0.29	-0.45	-0.14	1.00		
$C_0^{\rho\nabla J}$	0.37	-0.14	–	0.02	-0.00	–	0.44	-0.02	0.09	0.16	1.00	
$C_1^{\rho\nabla J}$	-0.06	-0.18	–	0.27	0.33	–	-0.38	-0.20	-0.01	0.00	-0.37	1.00
	ρ_c	E^{NM}/A	K^{NM}	$a_{\mathrm{sym}}^{\mathrm{NM}}$	$L_{\mathrm{sym}}^{\mathrm{NM}}$	$1/M_s^*$	$C_0^{\rho\Delta\rho}$	$C_1^{\rho\Delta\rho}$	V_0^n	V_0^p	$C_0^{\rho\nabla J}$	$C_1^{\rho\nabla J}$

Sensitivity analysis exhibits correlations of the model

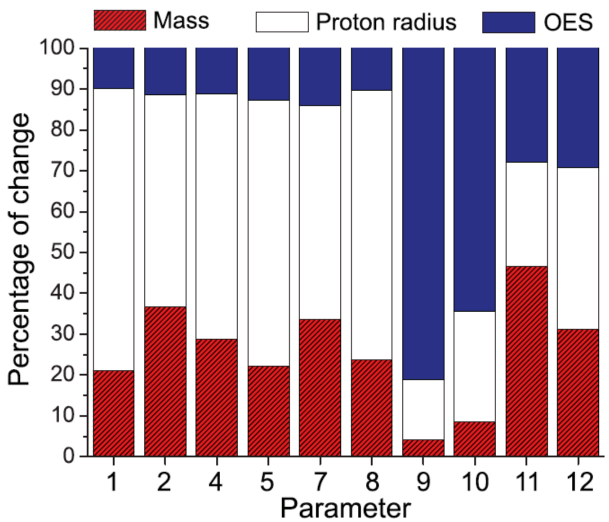

FIG. 10. (Color online) Sensitivity of the parameters of UNEDF0 to different data types entering χ^2. The EDF parameters are labeled as in Table VII.

← Sensitivity of parameters to changes in mass, proton radius, odd-even staggering [Kortelainen et al (2010)]

Correlation of observables within the model →
[Nazarewicz & Reinhard (2010)]

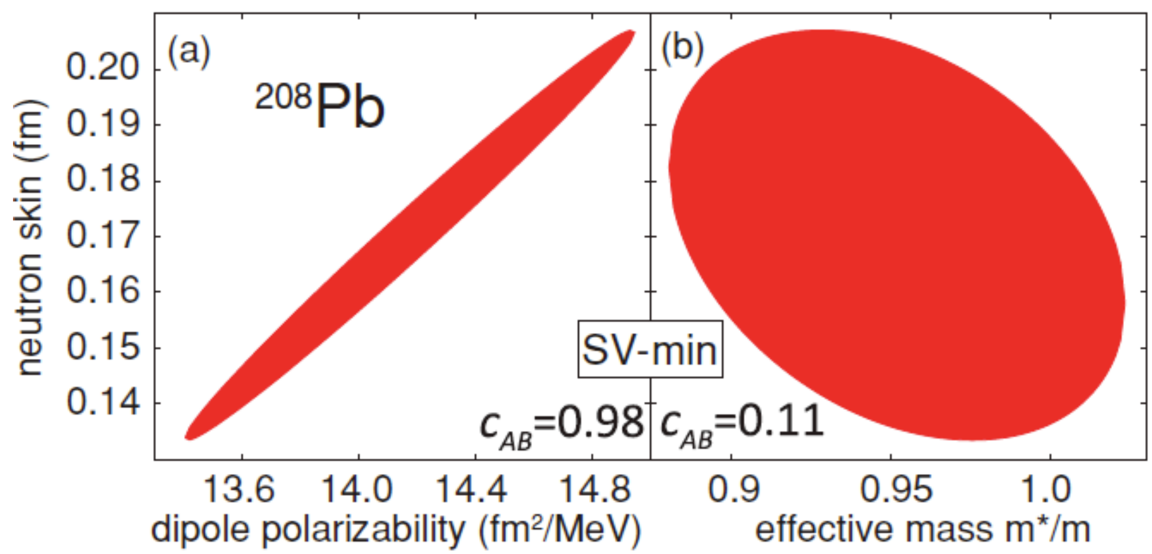

Dipole polarizability and neutron skin

$$\alpha_{\mathrm{D}} = \frac{8\pi}{9} e^2 \int_0^\infty \omega^{-1} R_{\mathrm{E1}}(\omega)\, d\omega$$

Correlations between observables based on an ensemble of ~18 functionals

$$C_{AB} = \frac{|\overline{\Delta A\, \Delta B}|}{\sqrt{\overline{\Delta A^2}\ \overline{\Delta B^2}}}$$

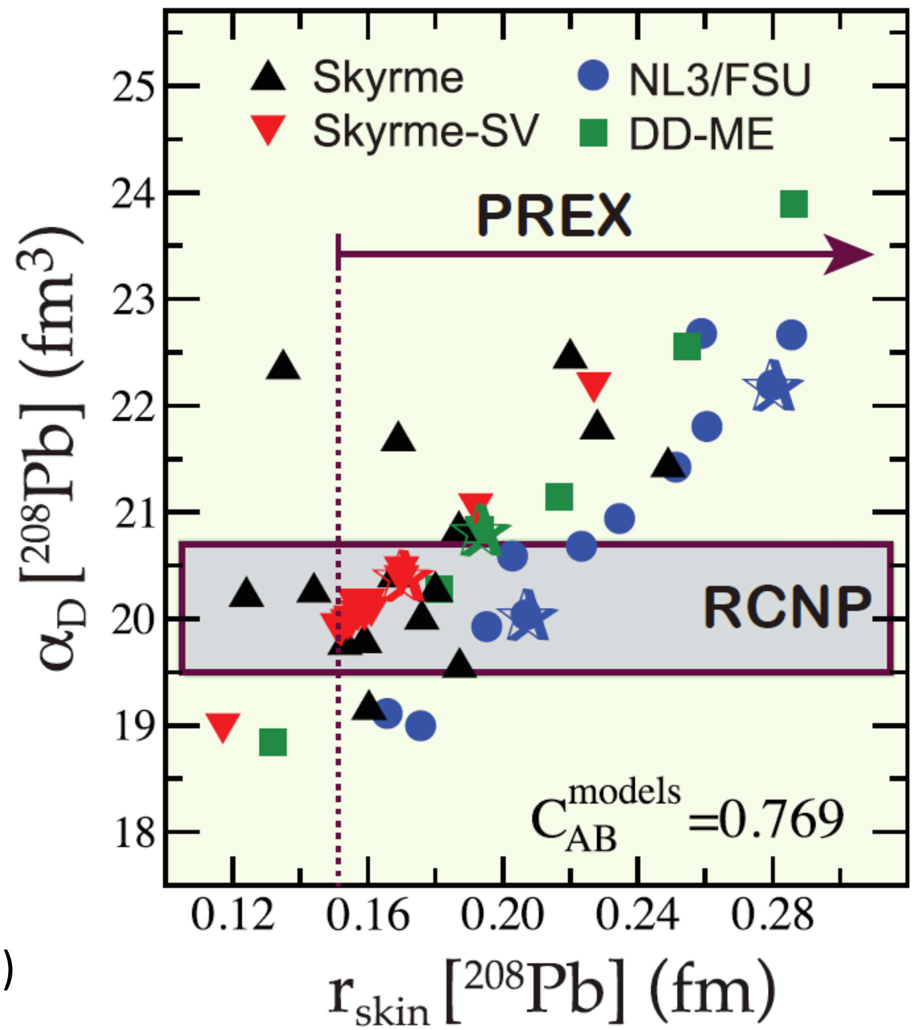

Tamii et al., Phys. Rev. Lett. 107, 062502 (2011);
Piekarewicz et al., Phys. Rev. C 85, 041302 (2012)

Strong correlations between neutron skins in different nuclei

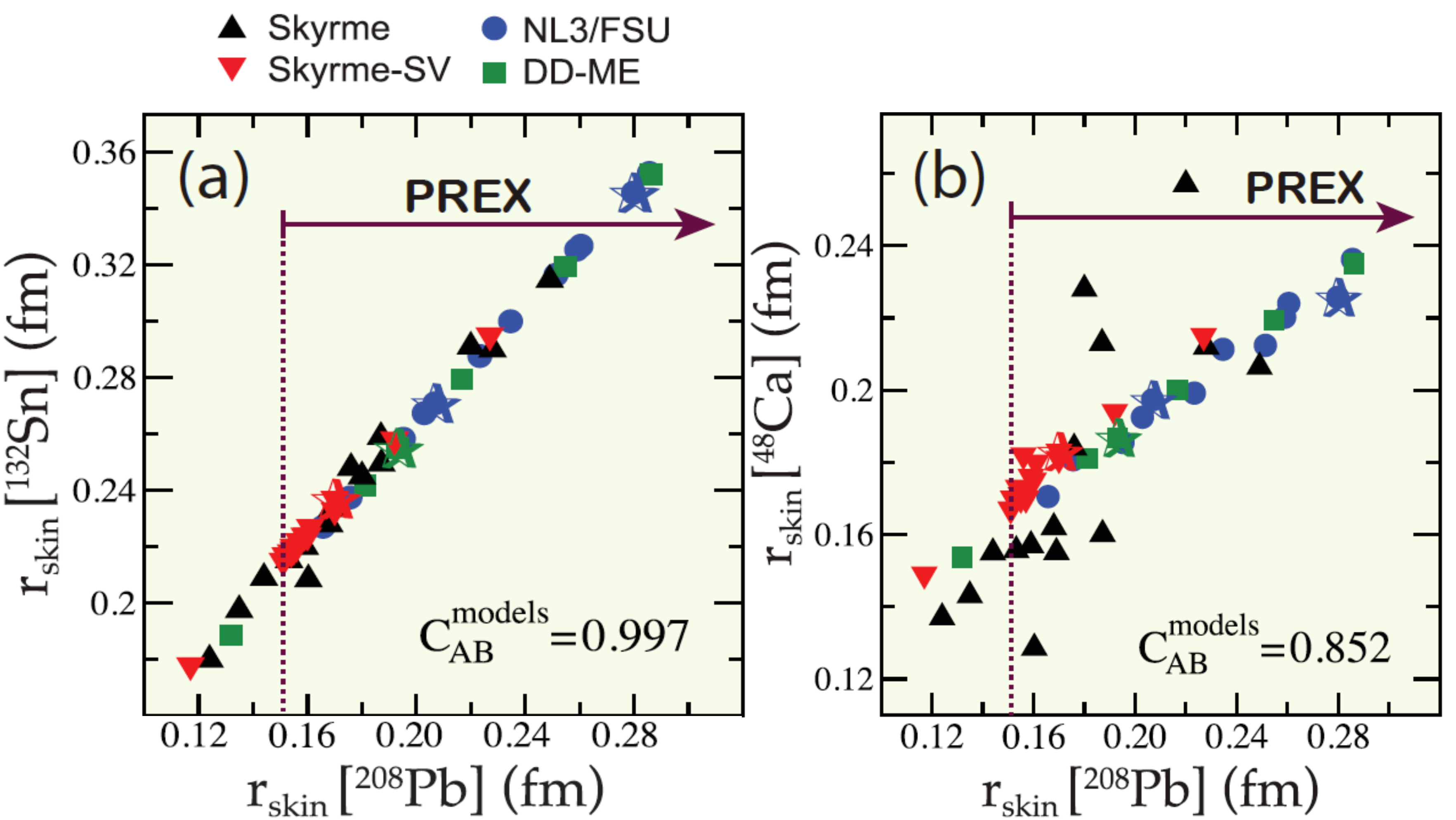

J. Piekarewicz et al., Phys. Rev. C 85, 041302(R) (2012)

UNEDF1

Enlarge set of opimization observables by excitation energies of fission isomers.

TABLE I. Experimental excitation energies of fission isomers [50] (in MeV) considered in the UNEDF1 data set.

Z	N	E
92	144	2.750
92	146	2.557
94	146	2.800
96	146	1.900

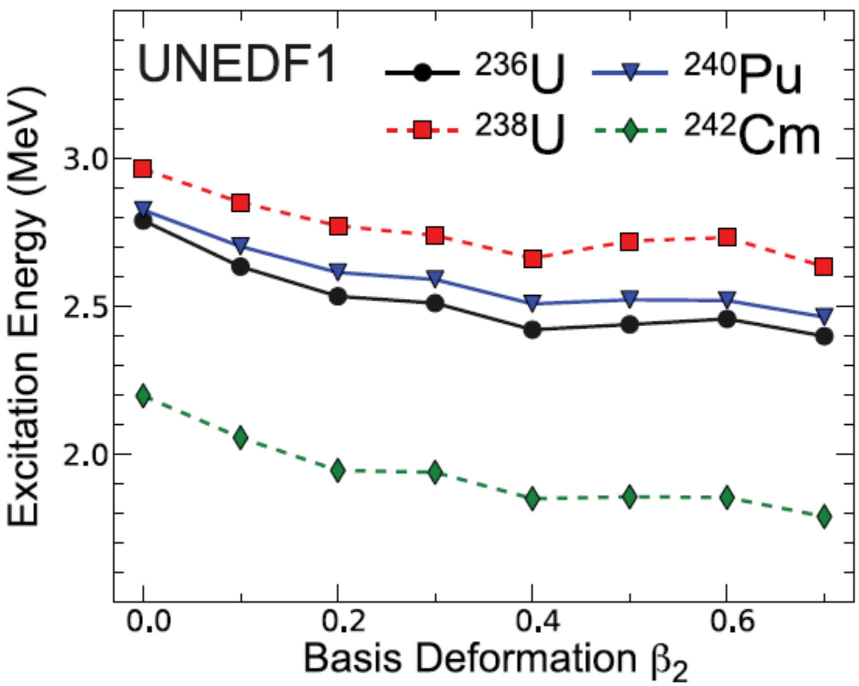

χ^2 comparisons

Observable	UNEDF0	UNEDF1	No.
E	1.428	1.912	555
E ($A < 80$)	2.092	2.566	113
E ($A \geqslant 80$)	1.200	1.705	442
S_{2n}	0.758	0.752	500
S_{2n} ($A < 80$)	1.447	1.161	99
S_{2n} ($A \geqslant 80$)	0.446	0.609	401
S_{2p}	0.862	0.791	477
S_{2p} ($A < 80$)	1.496	1.264	96
S_{2p} ($A \geqslant 80$)	0.605	0.618	381
$\tilde{\Delta}_n^{(3)}$	0.355	0.358	442
$\tilde{\Delta}_n^{(3)}$ ($A < 80$)	0.401	0.388	89
$\tilde{\Delta}_n^{(3)}$ ($A \geqslant 80$)	0.342	0.350	353
$\tilde{\Delta}_p^{(3)}$	0.258	0.261	395
$\tilde{\Delta}_p^{(3)}$ ($A < 80$)	0.346	0.304	83
$\tilde{\Delta}_p^{(3)}$ ($A \geqslant 80$)	0.229	0.248	312
R_p	0.017	0.017	49
R_p ($A < 80$)	0.022	0.019	16
R_p ($A \geqslant 80$)	0.013	0.015	33

Kortelainen et al., PRC C 85, 024304 (2012)

How many atomic nuclei exist?

Literature: 5,000-12,000

Skyrme-DFT: 6,900±500$_{syst}$

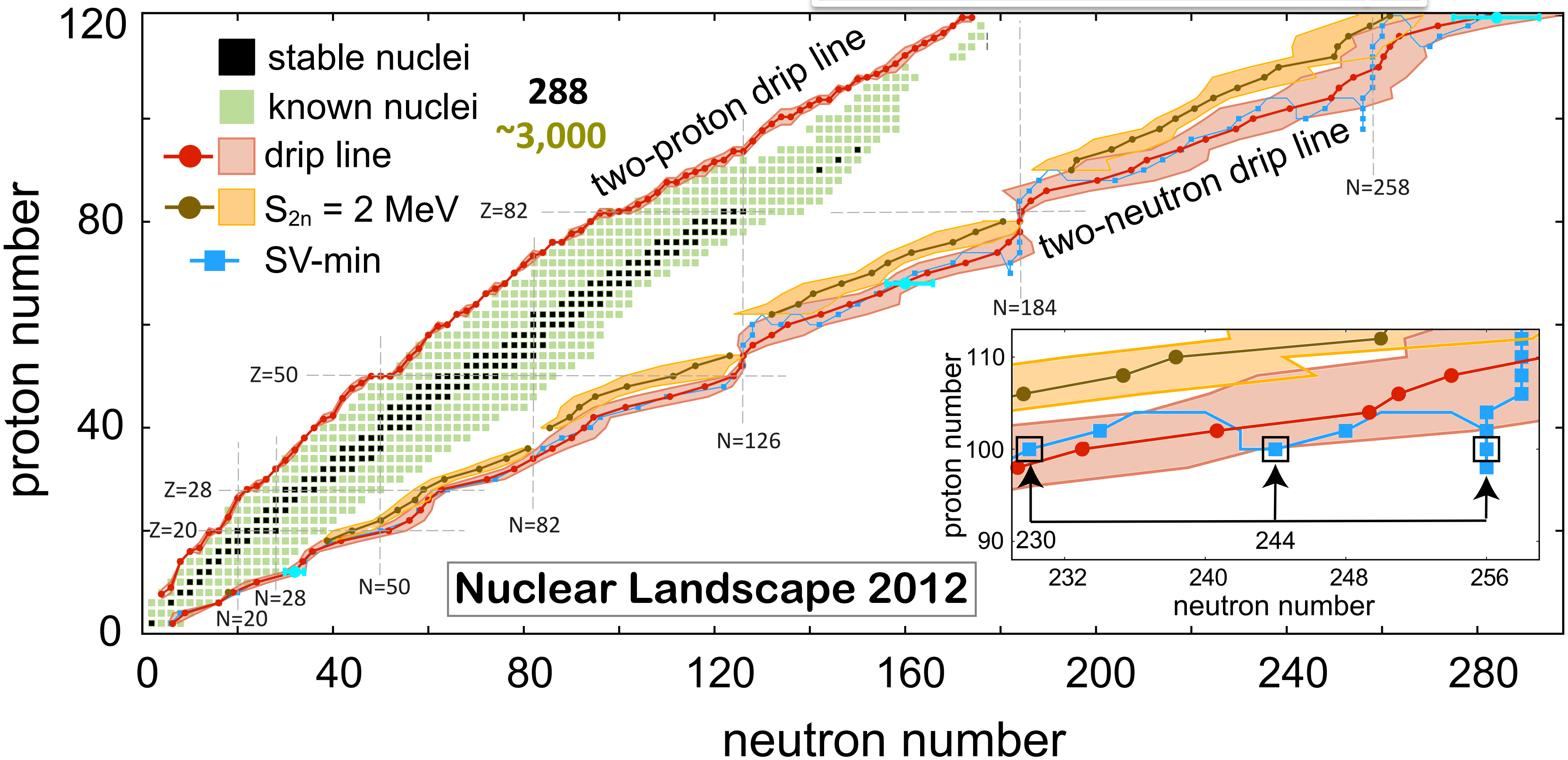

Models: SLy4, Svmin,UNEDF0, UNEDF1, FRDM and HFB-21

- Systematic errors (due to incorrect assumptions/poor modeling)
- Statistical errors (optimization and numerical errors)

Erler et al., Nature 486, 509 (2012)

Separation energies illustrate challenges

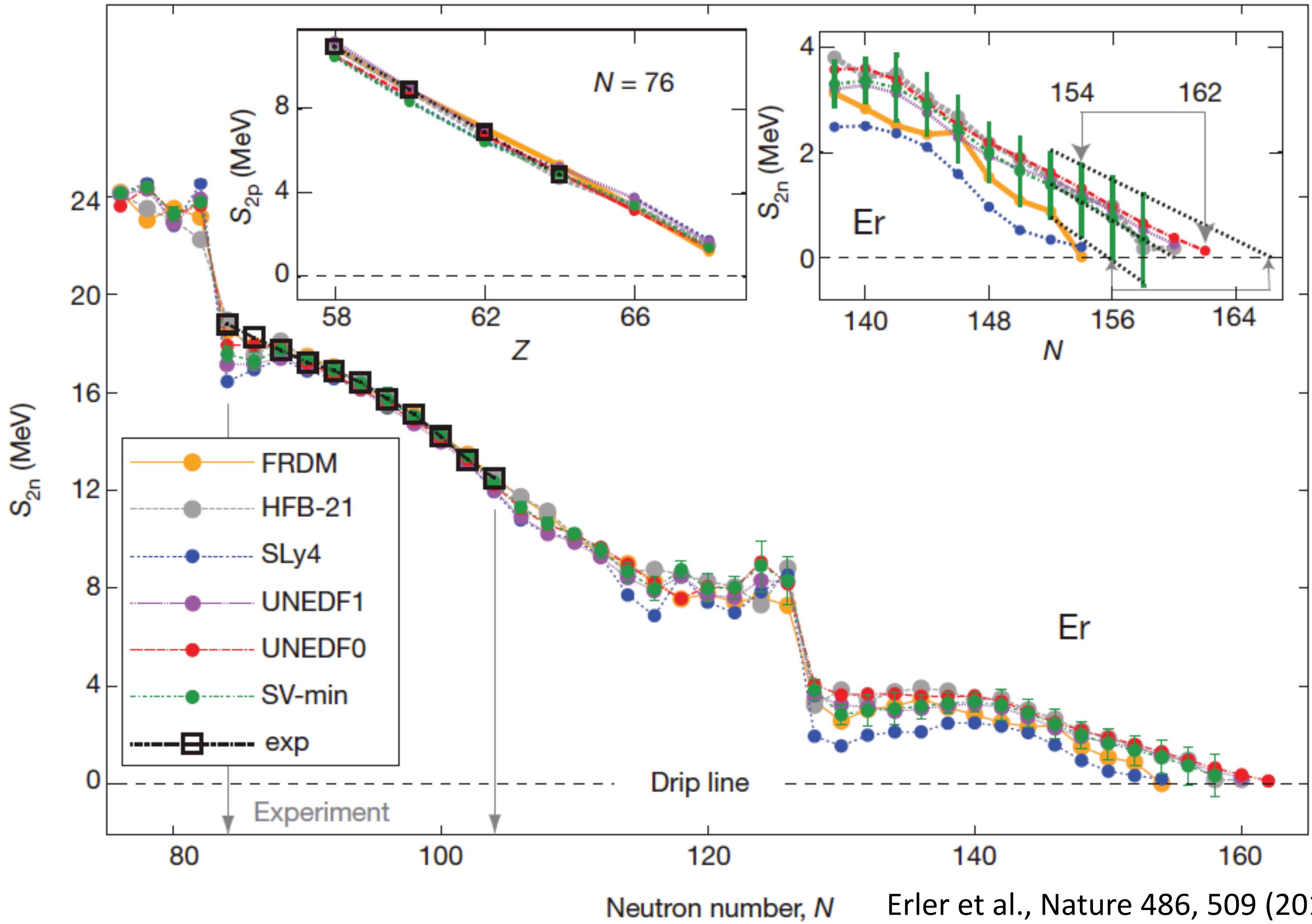

Erler et al., Nature 486, 509 (2012)

How many nuclei can be produced?

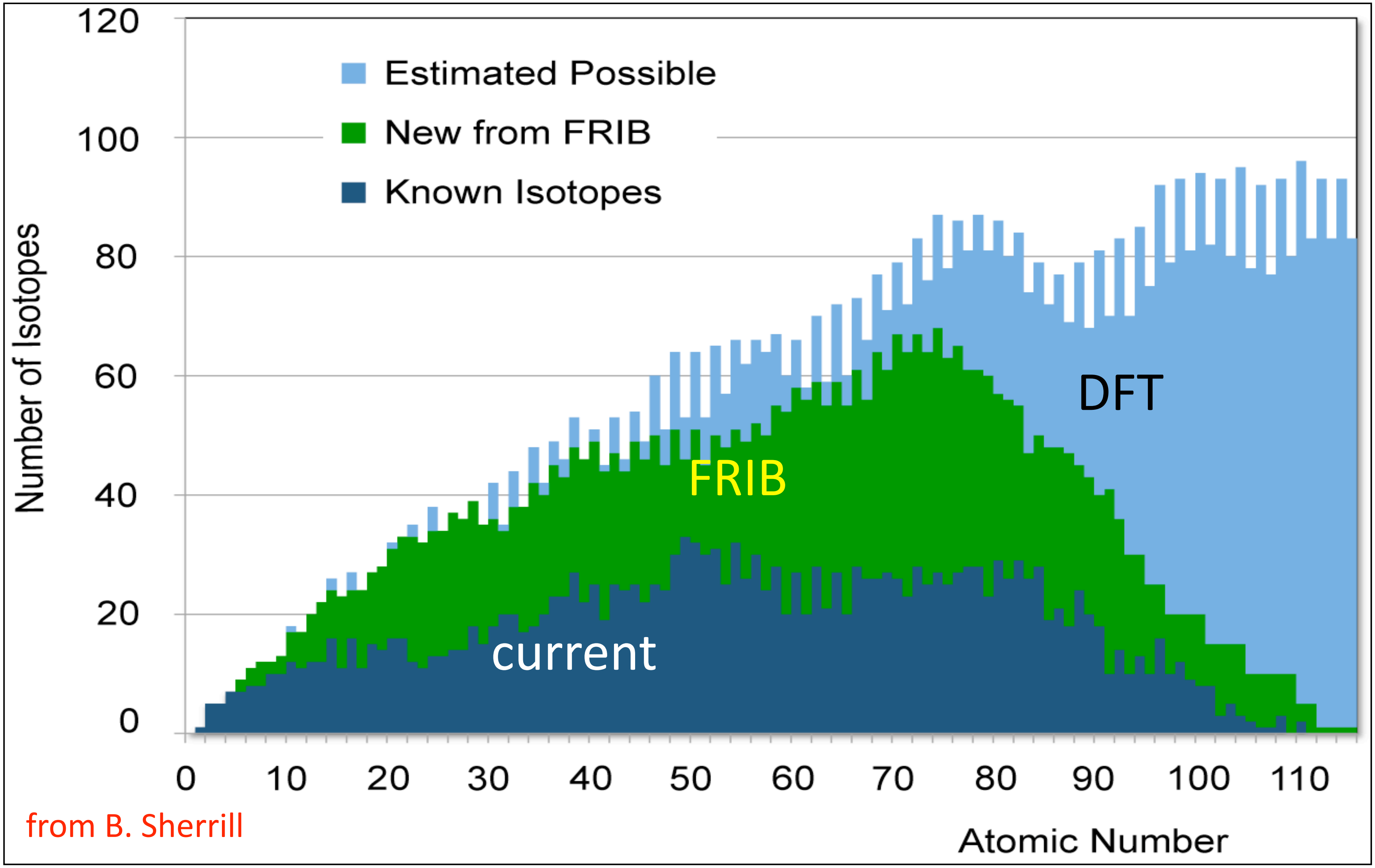

from B. Sherrill

Theoretical improvements of the energy functional: density-matrix expansion using soft interactions

Basic idea:
Vautherin & Negele (1972)

$$\rho\left(\vec{R}+\frac{\vec{s}}{2},\vec{R}-\frac{\vec{s}}{2}\right)=\rho_{SL}(sk_F)\rho(\vec{R})+\frac{35}{2sk_F^3}j_3(sk_F)[\tfrac{1}{4}\nabla^2\rho(\vec{R})-\tau(\vec{R})+\tfrac{3}{5}k_F^2\rho(\vec{R})]$$

Gebremariam, Duguet & Bogner (2010); J. W. Holt, Kaiser & Weise (2011)

$$\begin{aligned}\mathcal{H}_t^\pi(\boldsymbol{r}) = &\left(g_t^{\rho^2}(u)+\rho_0 h_t^{\rho^2}(u)\right)\rho_t^2\\ &+\left(g_t^{\rho\tau}(u)+\rho_0 h_t^{\rho\tau}(u)\right)\rho_t\tau_t\\ &+\left(g_t^{\rho\Delta\rho}(u)+\rho_0 h_t^{\rho\Delta\rho}(u)\right)\rho_t\Delta\rho_t\\ &+\left(g_t^{J^2}(u)+\rho_0 h_t^{J^2}(u)\right)J_t^2\\ &+\left(g_t^{\rho\nabla J}(u)+\rho_0 h_t^{\rho\nabla J}(u)\right)\rho_t\nabla J_t\end{aligned}$$

$$u = k_F/m_\pi \qquad\qquad k\equiv k_F(\boldsymbol{R})=\left(\frac{3\pi^2}{2}\rho_0(\boldsymbol{R})\right)^{1/3}$$

Short-range part is of Skyrme type but with a rich density-dependence in the couplings
(Long-ranged pion contributions not shown)

Discussion of nstabilities: Kortelainen & Lesinski, J. Phys. G 37 064039 (2010)

Density matrix expansion (pre optimization)

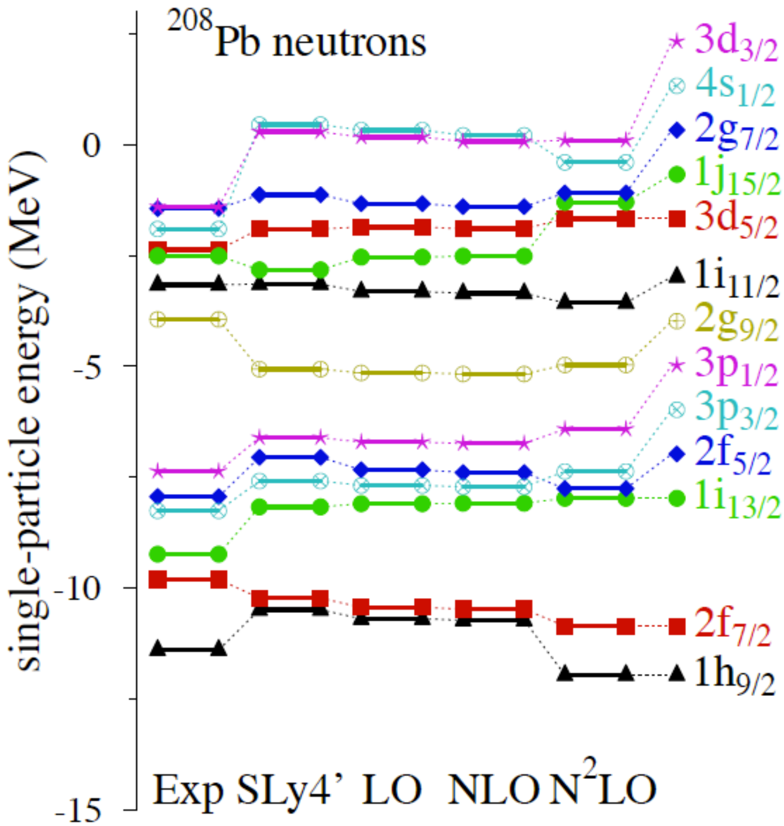

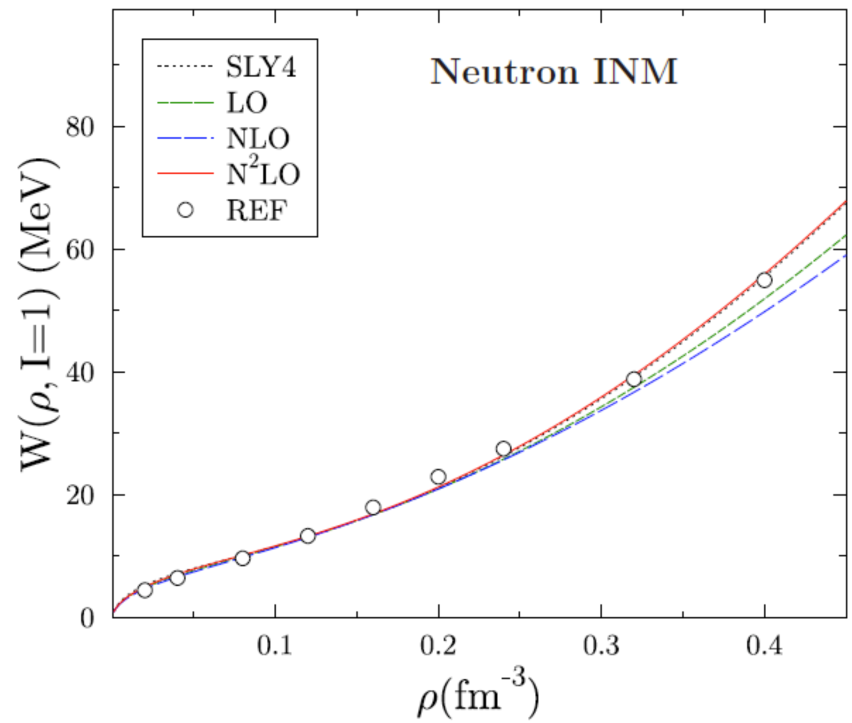

REF=Akmal, Pandharipande, Ravenhall, PRC 58, 1804 (1998).

Stoitsov, Kortelainen, Bogner, Duguet, Furnstahl, Gebremariam, Schunck, PRC 82, 054307 (2010)

Occupation-number based energy functional for nuclear masses

Inspiration: Mass formula by Duflo and Zuker (1995); RMS=0.35 MeV

[J. Mendoza-Temis, J. G. Hirsch, and A. P. Zuker, Nucl. Phys. A 843, 14 (2010).]

Functional: [M. Bertolli, TP, S.M. Wild, Phys. Rev. C 85, 014322 (2012)] RMS=1.31 MeV

Main idea: replace densities from Hohenberg-Kohn DFT by shell-model occupations

$$\rho(\mathbf{r}) \leftrightarrow n_\alpha$$

Functional:

$$F(c;n,z) = c_c \frac{Z(Z-1)}{A^{1/3}} + c_P \frac{\delta}{\sqrt{A}} + \mathcal{F}(c;n,z)$$

$$\begin{aligned}\mathcal{F}(c;n,z) \;=\; & \hbar\omega\Big(V + T_{\text{kin}} + I_{2\text{B}} + D \\ & + D_{4\text{B}} + \mathcal{T} + M_{4\text{Bex}} + L_{\text{val}}\Big) \\ & + \hbar\tilde{\omega}(\tilde{D}_{2\text{B}} + L + \tilde{L}).\end{aligned}$$

$$\begin{aligned} V &\equiv c_1 A, \\ T_{\text{kin}} &\equiv c_2 A^{-1/3} \sum_p p(z_p + n_p), \\ I_{2\text{B}} &\equiv c_3 A^{-1/3} \sum_p \left(\frac{z_p(z_p-1)}{p} \right. \\ & \qquad \left. + \frac{n_p(n_p-1)}{p} + \frac{2 n_p z_p}{p} \right), \\ D &\equiv c_4 \sum_p \left(\frac{\sqrt{d_p}}{2} - \frac{2}{d_p^{3/2}} (z_p - d_p/2)^2 \right) \\ & \qquad \times \sum_q \left(\frac{\sqrt{d_q}}{2} - \frac{2}{d_q^{3/2}} (n_q - d_q/2)^2 \right), \end{aligned}$$

Adjust 17 parameters

$$c \equiv \{c_1, c_2, \ldots, c_{11}, c_c, c_P, c_s, c_{as}, c_{ss}, \tilde{c}_s\}$$

by globally optimizing functional to 2049 masses

Results: RMS deviation from data is 1.31 MeV

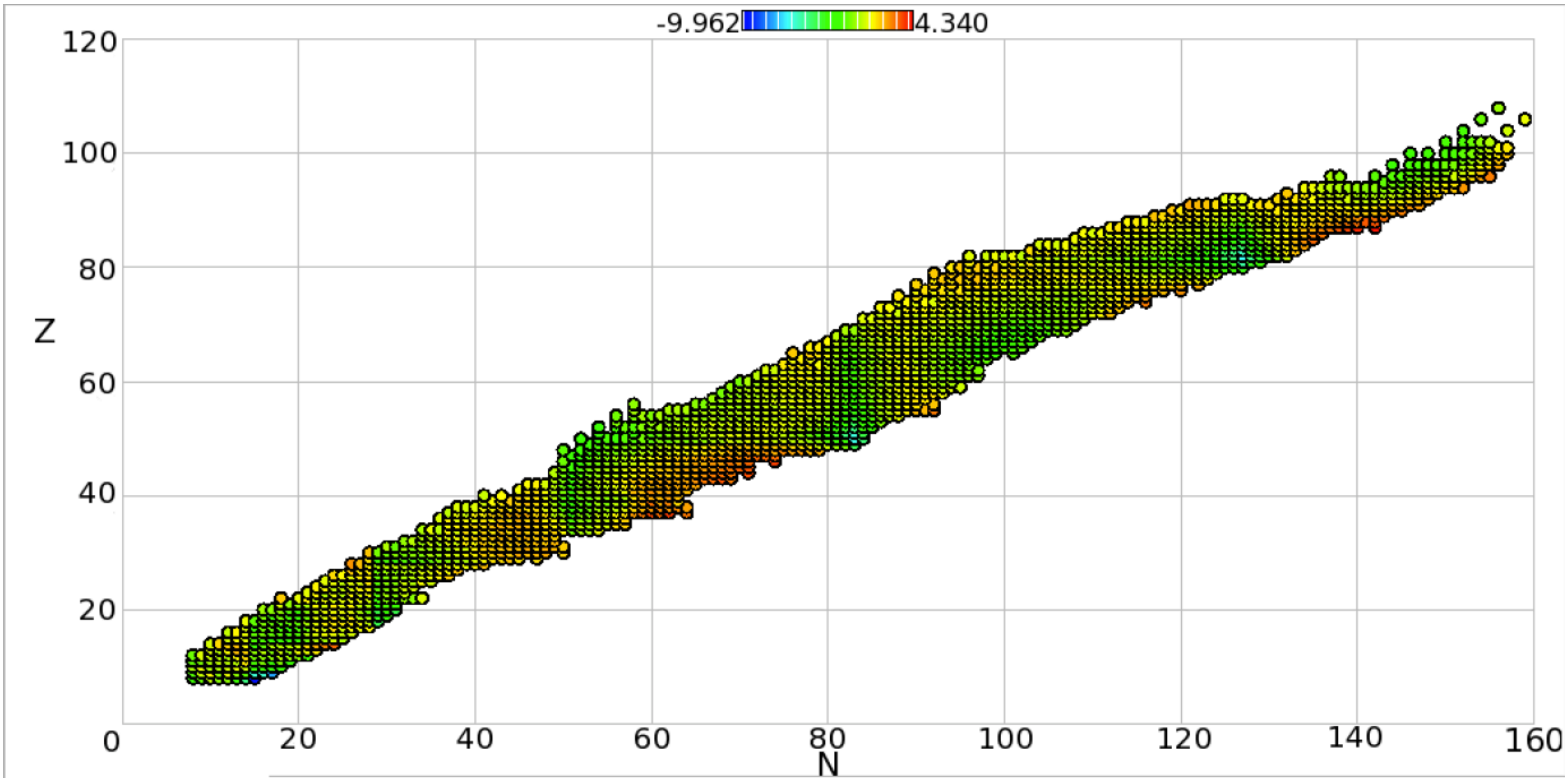

Deviations smooth across the nuclear chart
Some shell oscillations / deformations visible

Results: deviations from data as a function of N

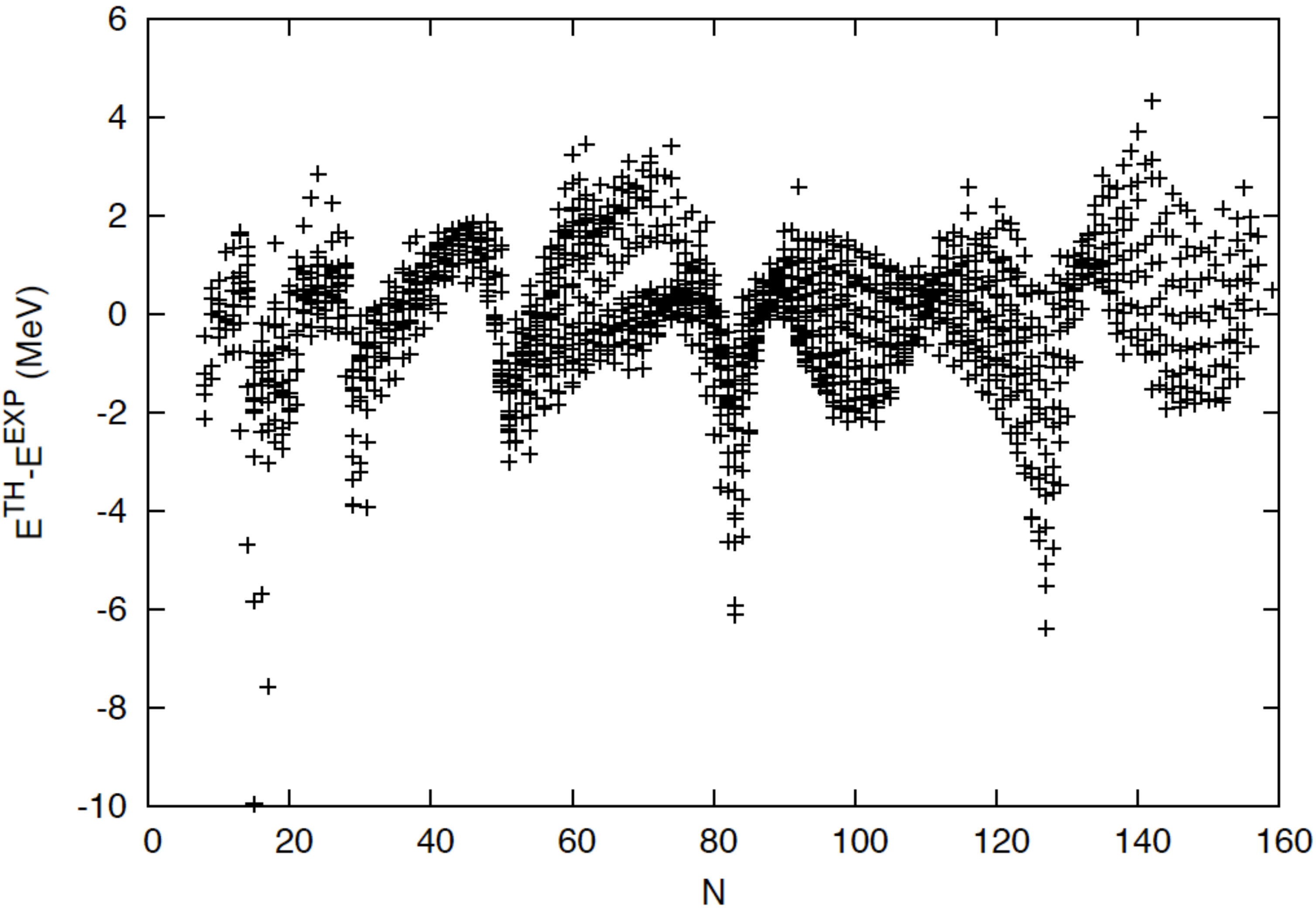

Deformations vs. shell closures

Extrapolation properties of the functional

Data Set	N_{pts}	χ (MeV)		
		Fit	Extrapolation to	
			Data Set B	Data Set C
A	1837	1.38	1.34	1.40
B	2049	1.31	–	1.38
C	2149	1.37	–	–

Data sets:

A: 1995 data set
B: well-determined nuclei (exp. uncertainty < 0.2MeV) from 2003 data set
C: Full 2003 data set

Functional extrapolates reasonably well

Evolution of shell structure in calcium

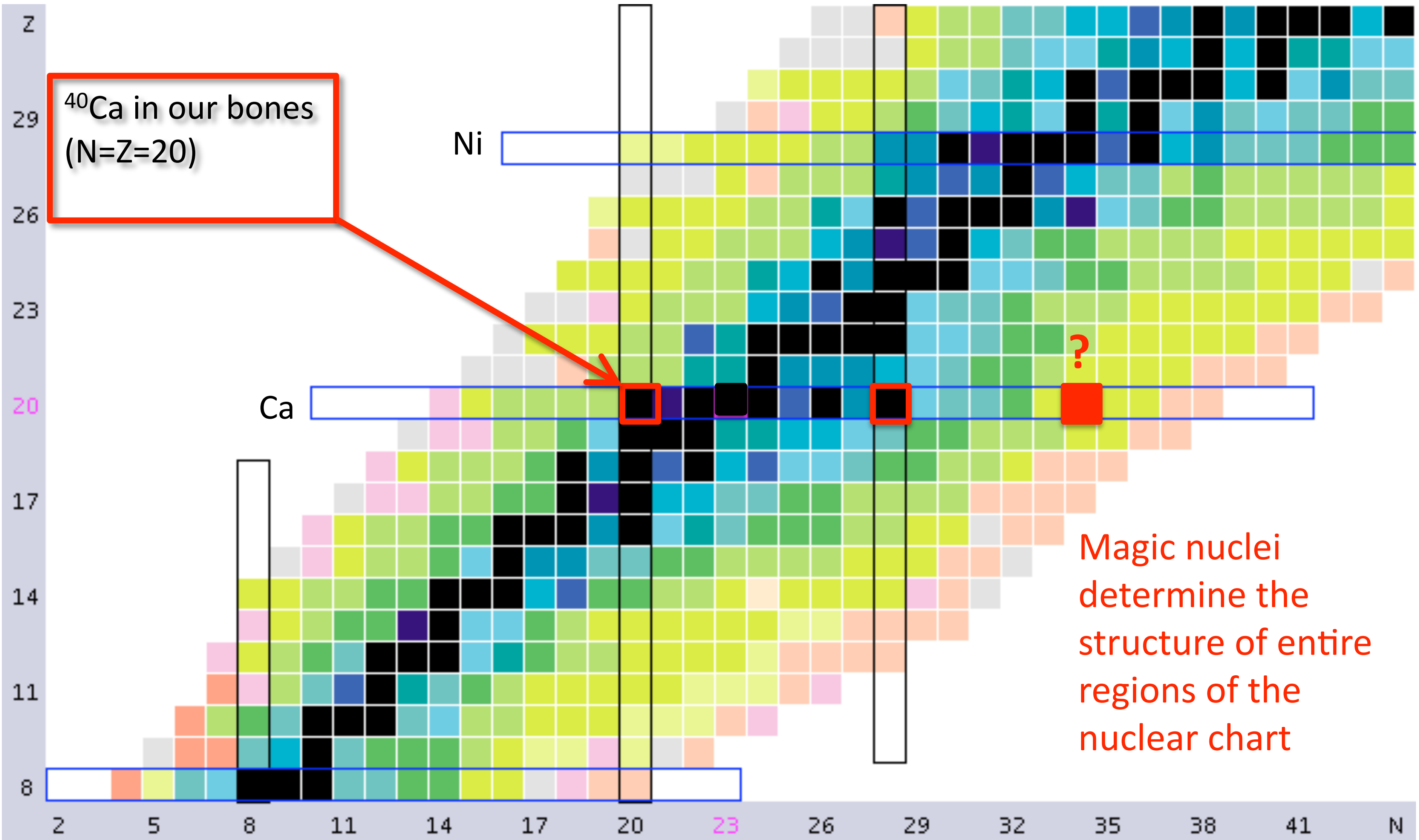

Shell evolution from relativistic mean-field

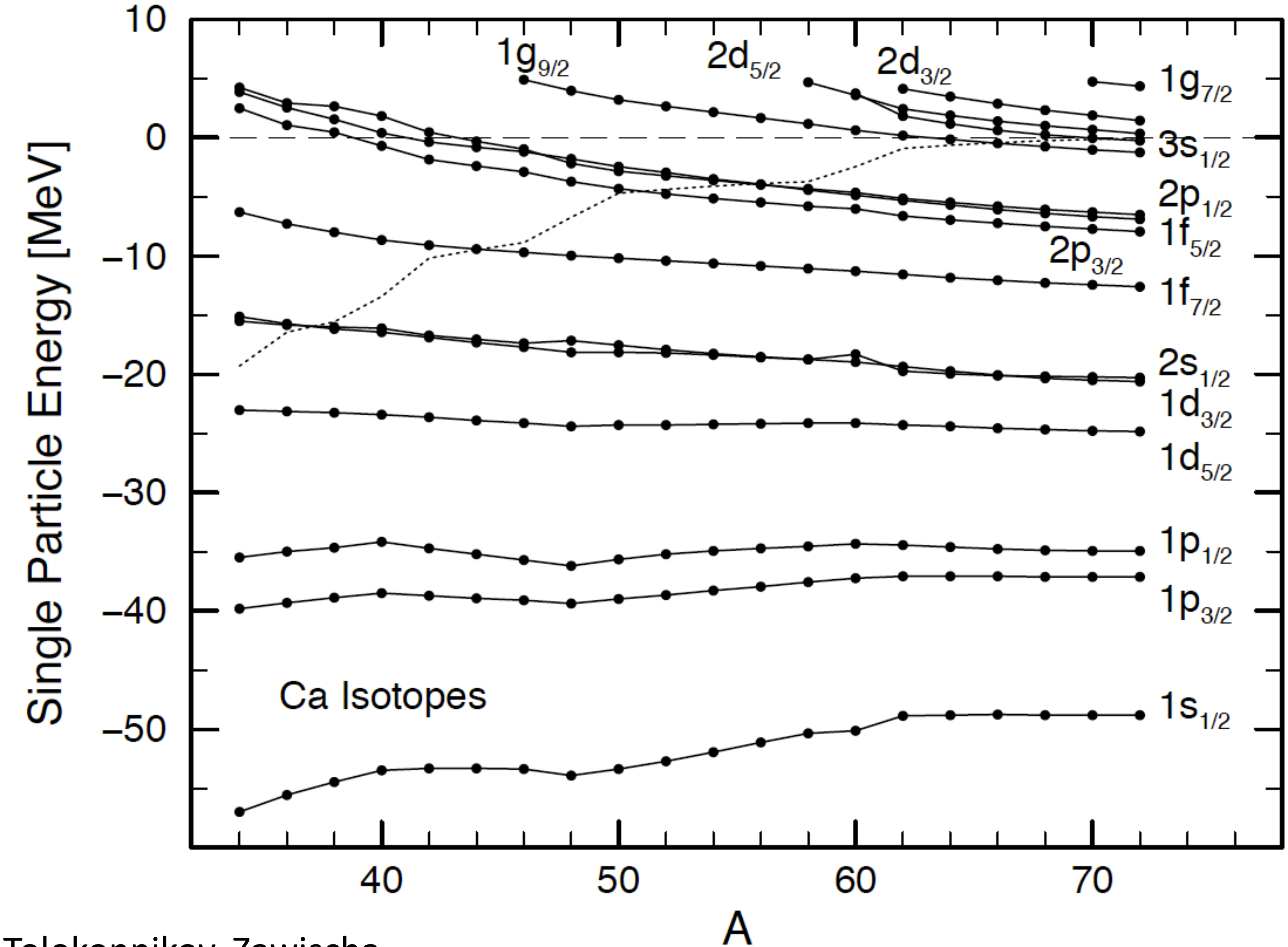

Fayans, Tolokonnikov, Zawischa,
Phys. Lett. B 491, 245 (2000)

J. Meng et al., PRC 65, 041302(R) (2002)

Shell model

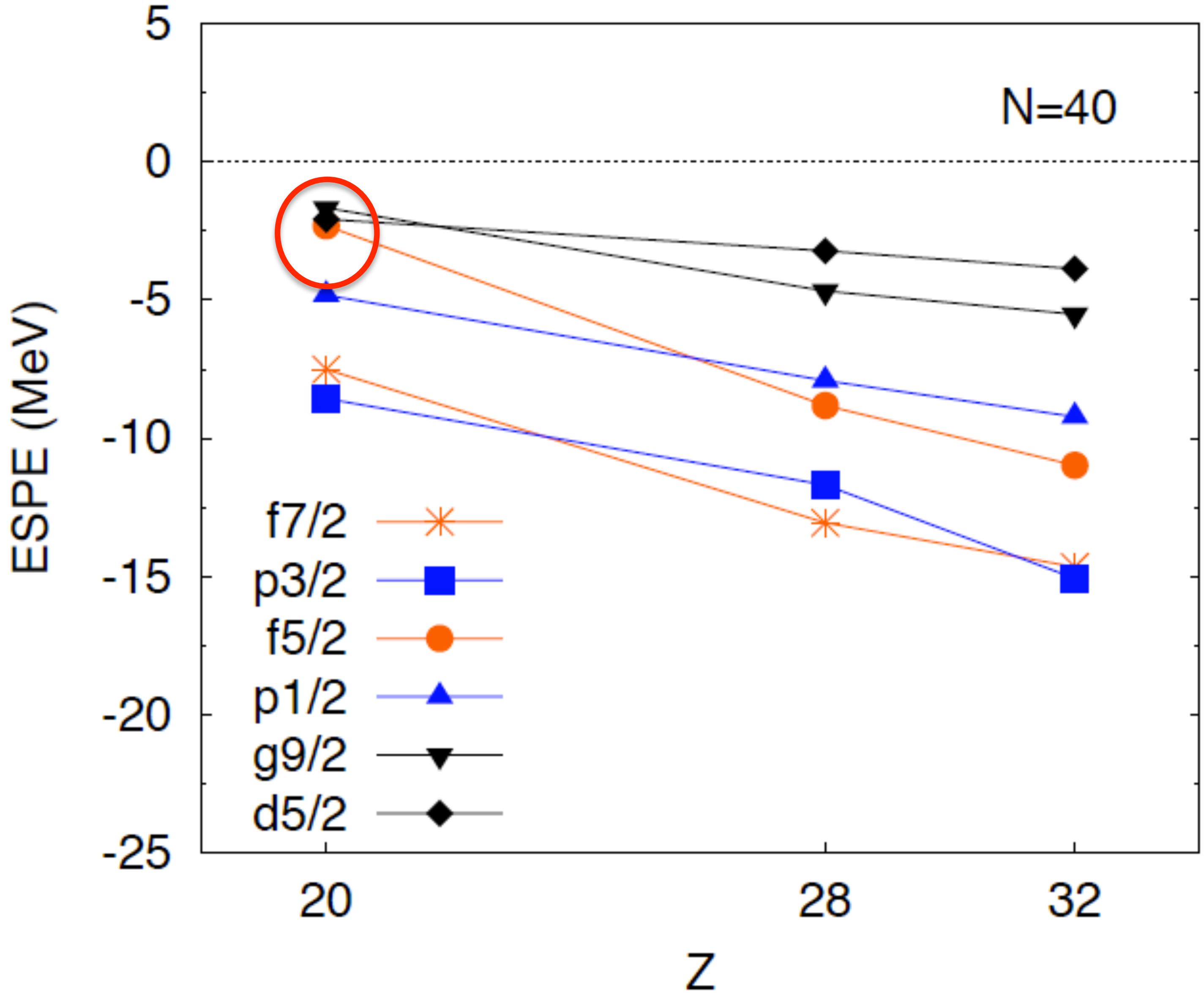

S. M. Lenzi, F. Nowacki, A. Poves, K. Sieja, PRC 82 054301 (2010).

Is ^{54}Ca a magic nucleus? (Is N=34 a magic number?)

Results from coupled-cluster computations with NN forces from chiral EFT and in-medium effective 3NF: k_F=0.95 fm^{-1}, c_E=0.735, c_D=-0.2
[Holt, Kaiser, Weise 2009; Hebeler and Schwenk 2010]

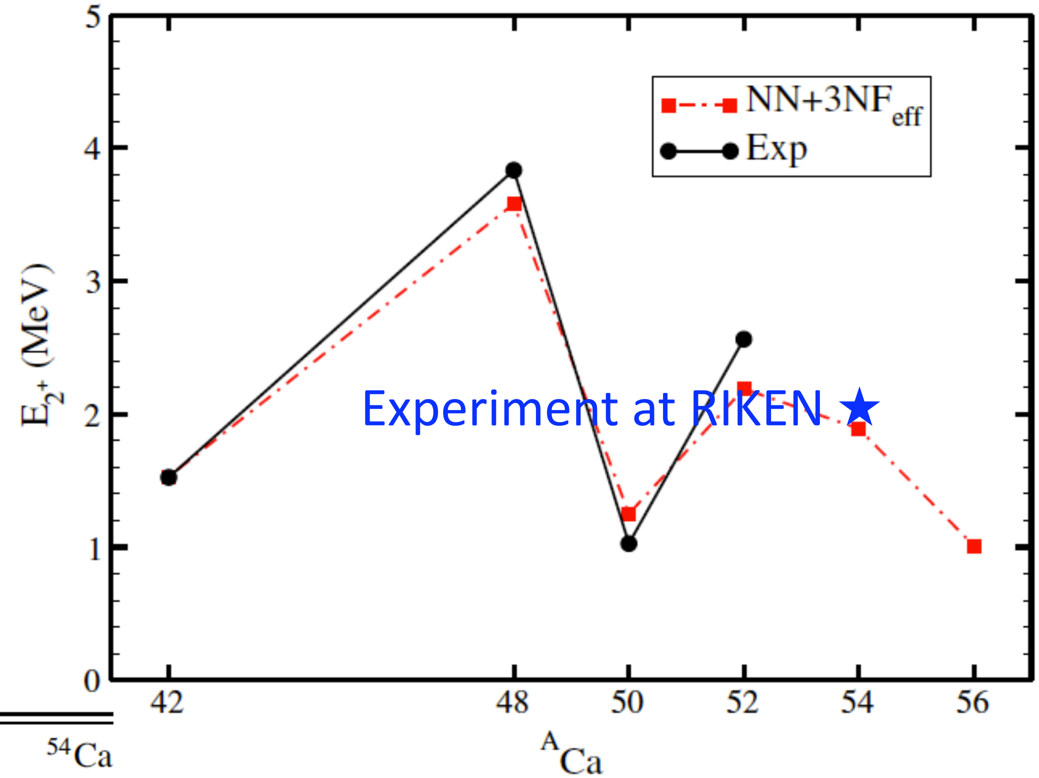

^{54}Ca exhibits soft subshell closure

Measurement at RIKEN (Japan) agrees with theoretical prediction.

	^{48}Ca	^{52}Ca	^{54}Ca
E_{2^+} (CC) (MeV)	3.58	2.19	1.89
E_{2^+} (Expt) (MeV)	3.83	2.56	n.a.[a]
E_{4^+}/E_{2^+} (CC)	1.17	1.80	2.36
E_{4^+}/E_{2^+} (Expt)	1.17	n.a.	n.a.
S_n (CC) (MeV)	9.45	6.59	4.59
S_n (Expt) (MeV)	9.95	6.0[b]	4.0[c]

Recent mass measurement by Gallant et al., Phys. Rev. Lett. **109,** 032506 (2012)

Hagen, Hjorth-Jensen, Jansen, Machleidt,TP, Phys. Rev. Lett. 109 032502 (2012)

Binding energies and spectra of Ca isotopes

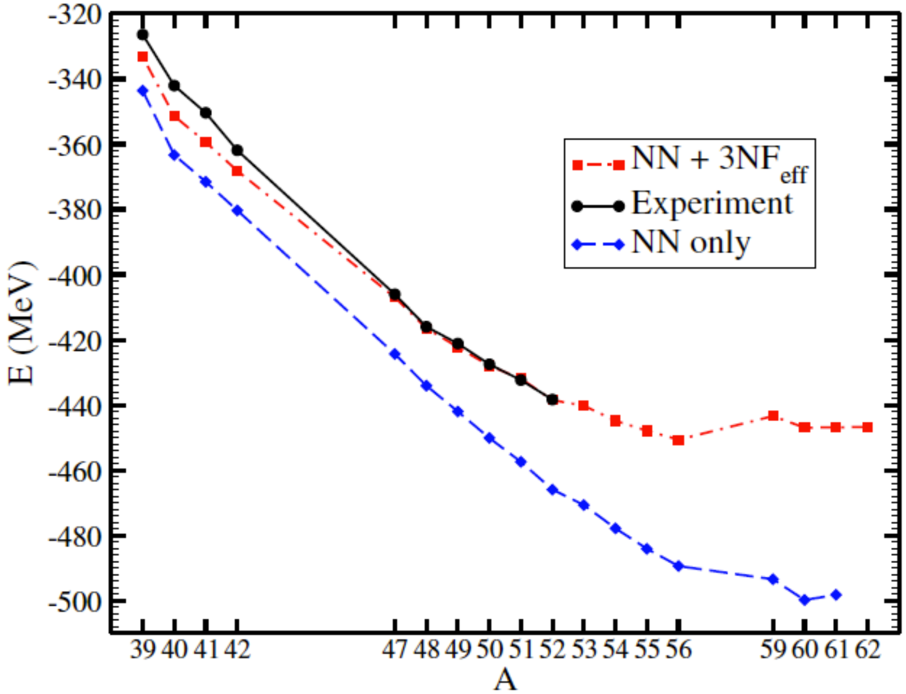

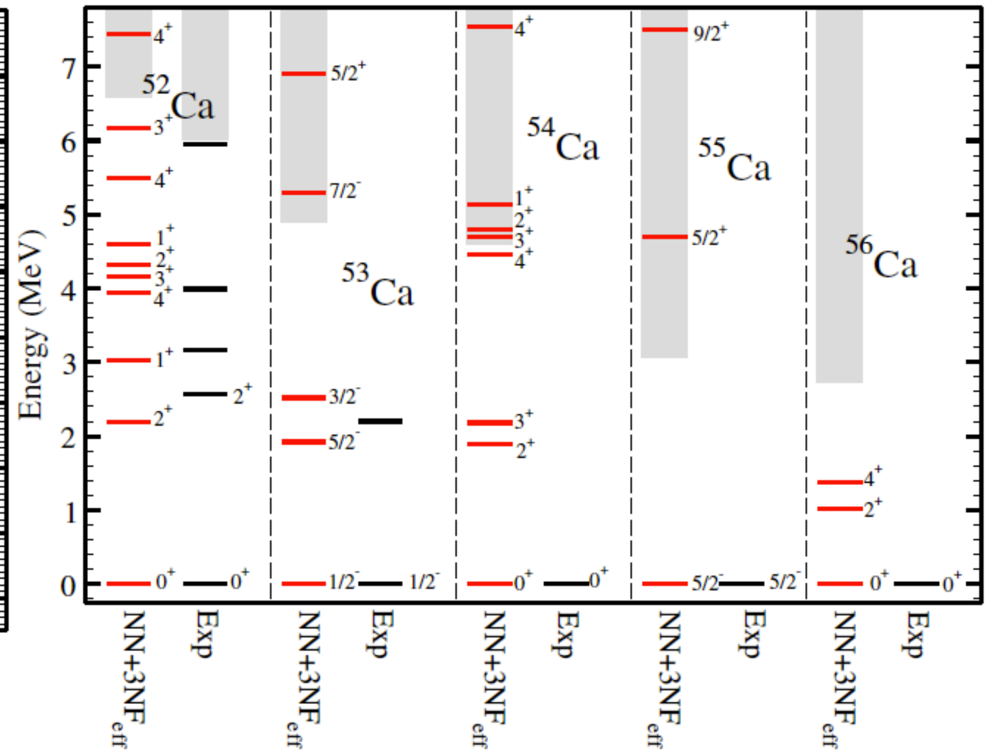

Results

- Effective chiral 3NF acts repulsive
- In ^{61}Ca, level ordering $s_{1/2}$, $d_{5/2}$, $g_{9/2}$
- ^{48}Ca magic due to 3NF [J. D. Holt et al, J. Phys. G 39, 085111 (2012)]
- Dripline beyond ^{60}Ca?

	^{53}Ca		^{55}Ca		^{61}Ca	
J^π	Re[E]	Γ	Re[E]	Γ	Re[E]	Γ
$5/2^+$	1.99	1.97	1.63	1.33	1.14	0.62
$9/2^+$	4.75	0.28	4.43	0.23	2.19	0.02

Hagen, Hjorth-Jensen, Jansen, Machleidt, TP, Phys. Rev. Lett. 109 032502 (2012)

Optimization of chiral interaction an NNLO

A. Ekström, G. Baardsen, C. Forssen, G. Hagen, M. Hjorth-Jensen, G. R. Jansen, R. Machleidt, W. Nazarewicz, TP, J. Sarich, S. M. Wild, arXiv:1303.4674

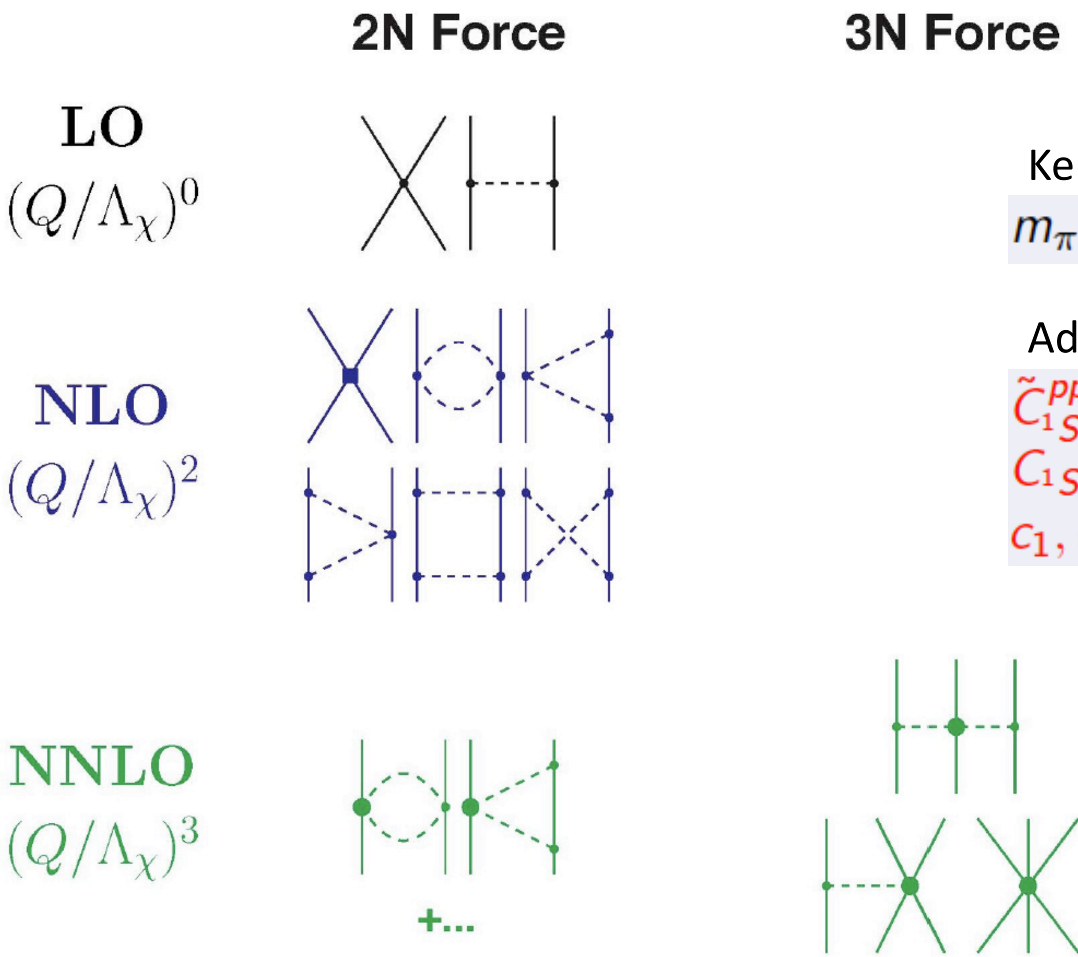

Kept fixed

$m_{\pi^+}, m_{\pi^-}, m_{\pi^0}, m_n, m_p, g_A, f_\pi, \Lambda_{LS}, \Lambda_\chi$

Adjusted parameters

$\tilde{C}^{pp}_{^1S_0}, \tilde{C}^{nn}_{^1S_0}, \tilde{C}^{np}_{^1S_0}, \tilde{C}_{^3S_1}$
$C_{^1S_0}, C_{^3P_0}, C_{^1P_1}, C_{^3P_1}, C_{^3S_1}, C_{^3S_1-^3D_1}, C_{^3P_2}$
$c_1, c_3, c_4, (c_D, c_E)$

Weinberg; van Kolck; Epelbaum, Glöckle & Meiβner; Entem & Machleidt; …

Optimization to phase shifts; χ^2 from data

$$f(\vec{x}) = \sum_{q=1}^{N_q} \left(\frac{\delta_q^{\mathrm{NNLO}}(\vec{x}) - \delta_q^{\mathrm{Nijm93}}}{w_q} \right)^2$$

πN LEC	πN-scattering[1]	NN-PWA[2]	NNLO[3]	N3LO	POUNDerS
c_1 [GeV^{-1}]	-0.81±0.15	-0.76±0.07	-0.81	-0.81	-0.9186
c_3 [GeV^{-1}]	-4.69±1.34	-4.78±0.10	-3.40	-3.20	-3.8887
c_4 [GeV^{-1}]	+3.40±0.04	+3.96 ±0.22	+3.40	+5.40	+4.3103

[1] πN Fit 1, in P. Büttiker, U-G. Meißner Nucl. Phys. A **668**, 97 (2000)
[2] *NN* PWA, in M. C. M. Rentmeester *et al.* Phys. Rev C **67** 044001 (2003)

[3] E. Epelbaum et al., Eur. Phys. J. A19, 401 (2004)

χ^2/datum, *np* scattering data (1999 database)

The previous picture...

T_{lab} bin (MeV)	N3LO	NNLO[1]	NLO[1]	AV18
0-100	1.06	1.71	5.20	0.95
100-190	1.08	12.9	49.3	1.10
190-290	1.15	19.2	68.3	1.11
0-290	**1.10**	**10.1**	**36.2**	**1.04**

[1] E. Epelbaum et al., Eur. Phys. J. A19, 401 (2004)

... changes with POUNDerS

T_{lab} bin (MeV)	POUNDerS-NNLO(500)
0-35	0.85
35-125	1.17
125-183	1.87
183-290	6.09
0-290	**2.95**

χ^2/datum, *pp* scattering data (1999 database)

The previous picture...

T_{lab} bin (MeV)	N3LO	NNLO[1]	NLO[1]	AV18
0-100	1.05	6.66	57.8	0.96
100-190	1.50	28.3	62.0	1.31
190-290	1.93	66.8	111.6	1.82
0-290	**1.50**	**35.4**	**80.1**	**1.38**

[1] E. Epelbaum et al., Eur. Phys. J. A19, 401 (2004)

... changes with POUNDerS

T_{lab} bin (MeV)	POUNDerS-NNLO(500)
0-35	1.11
35-125	1.56
125-183	23.95 (4.35[a])
183-290	29.26
0-290	**17.10 (14.03)**[2]

[2] Total (0-290) MeV *pp* χ^2/datum when excluding two low-uncertainty data sets.

Optimization with POUNDerS

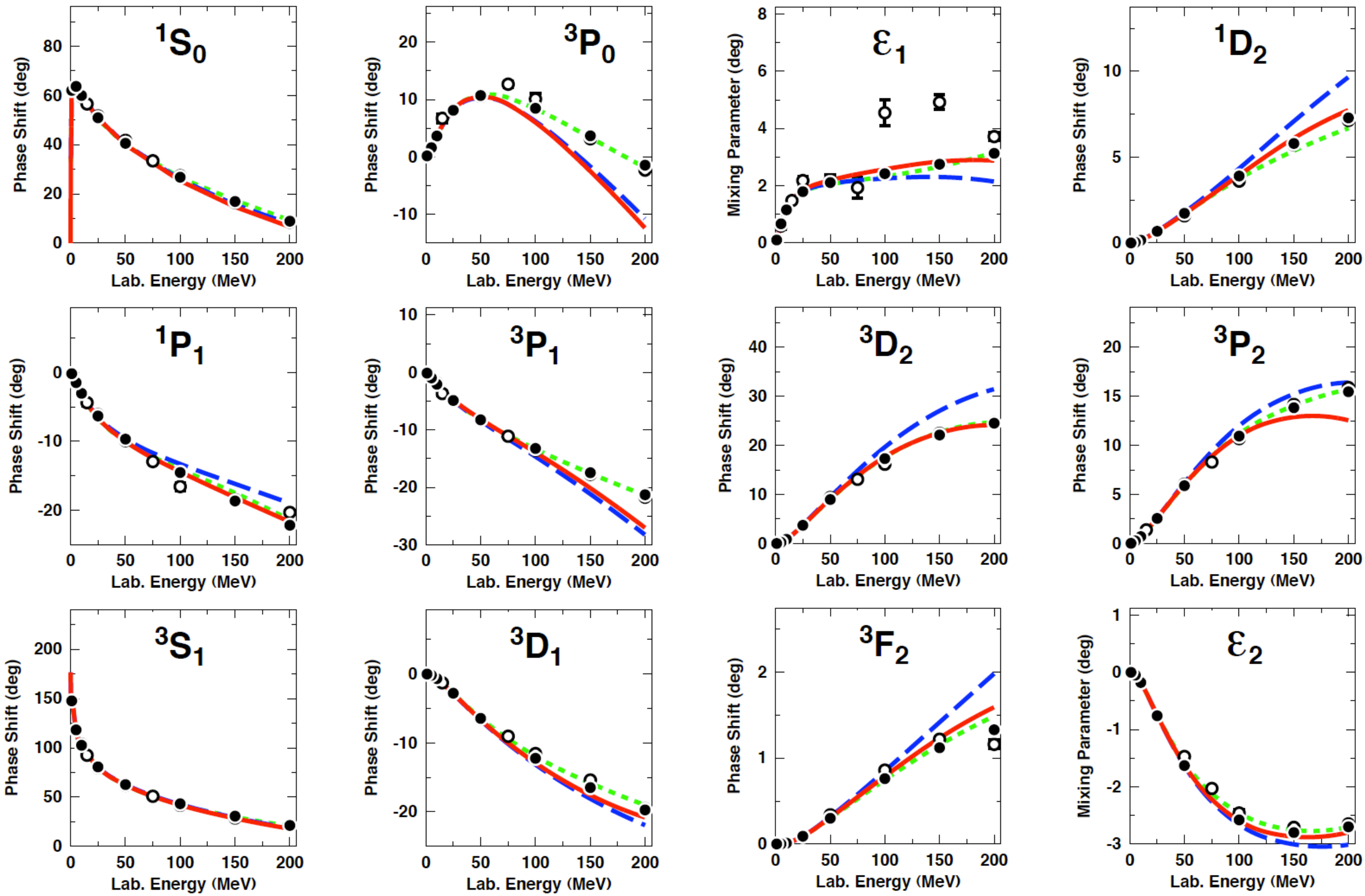

Nucleon-nucleon properties

	N^3LO_{EM}	$NNLO_{opt}$	Exp.
a^C_{pp}	-7.8188	-7.8174	-7.8196(26) -7.8149(29)
r^C_{pp}	2.795	2.755	2.790(14) 2.769(14)
a^N_{pp}	-17.083	-17.825	
r^N_{pp}	2.876	2.817	
a_{nn}	-18.900	-18.889	-18.95(40)
r_{nn}	2.838	2.797	2.75(11)
a_{np}	-23.732	-23.749	-23.740(20)
r_{np}	2.725	2.684	2.77(5)
B_D (MeV)	2.224575	2.224582	2.224575(9)
r_D (fm)	1.975	1.967	1.97535(85)
Q_D (fm^2)	0.275	0.272	0.2859(3)
P_D (%)	4.51	4.05	

Oxygen isotopes (NN only)

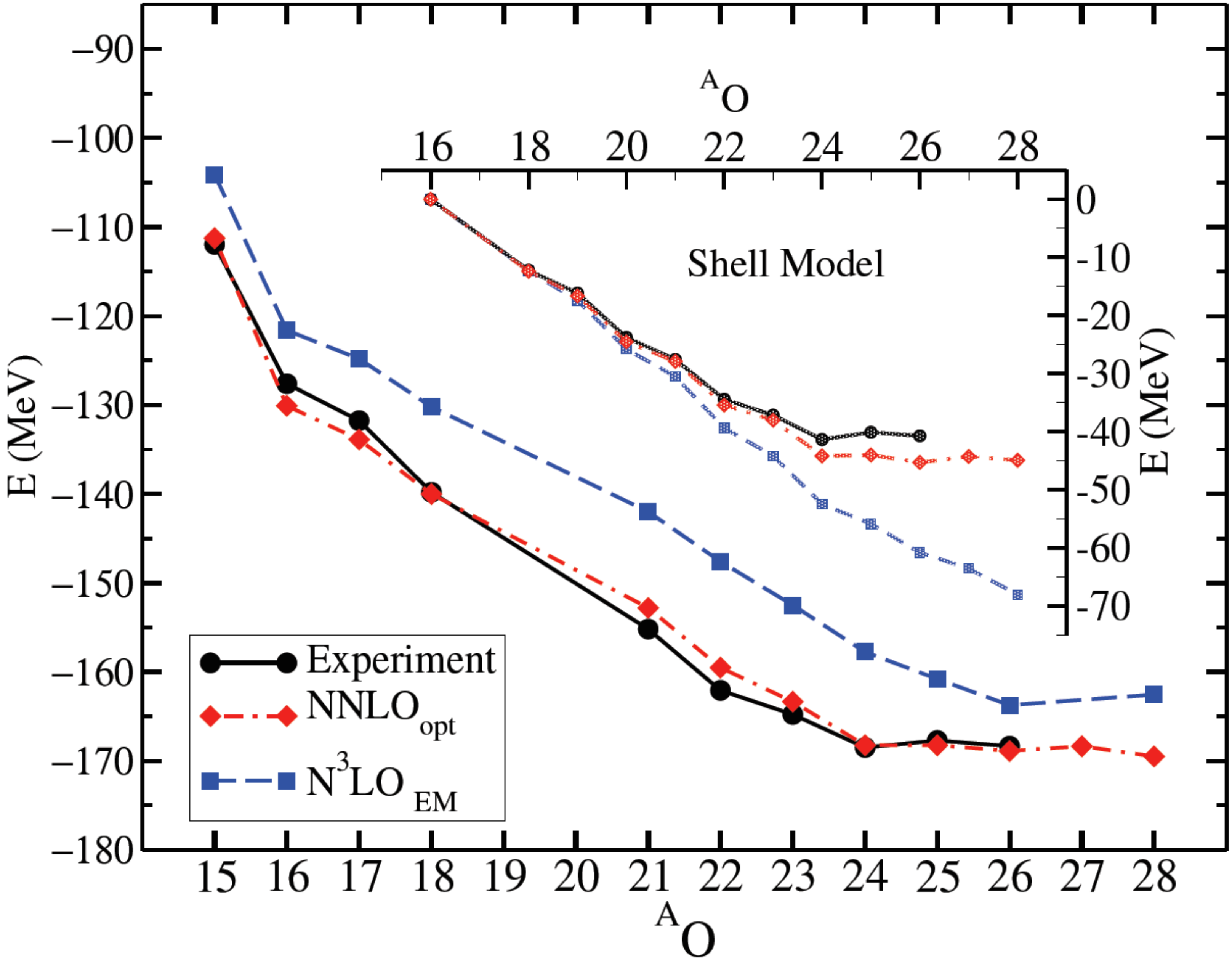

Calcium isotopes (NN only)

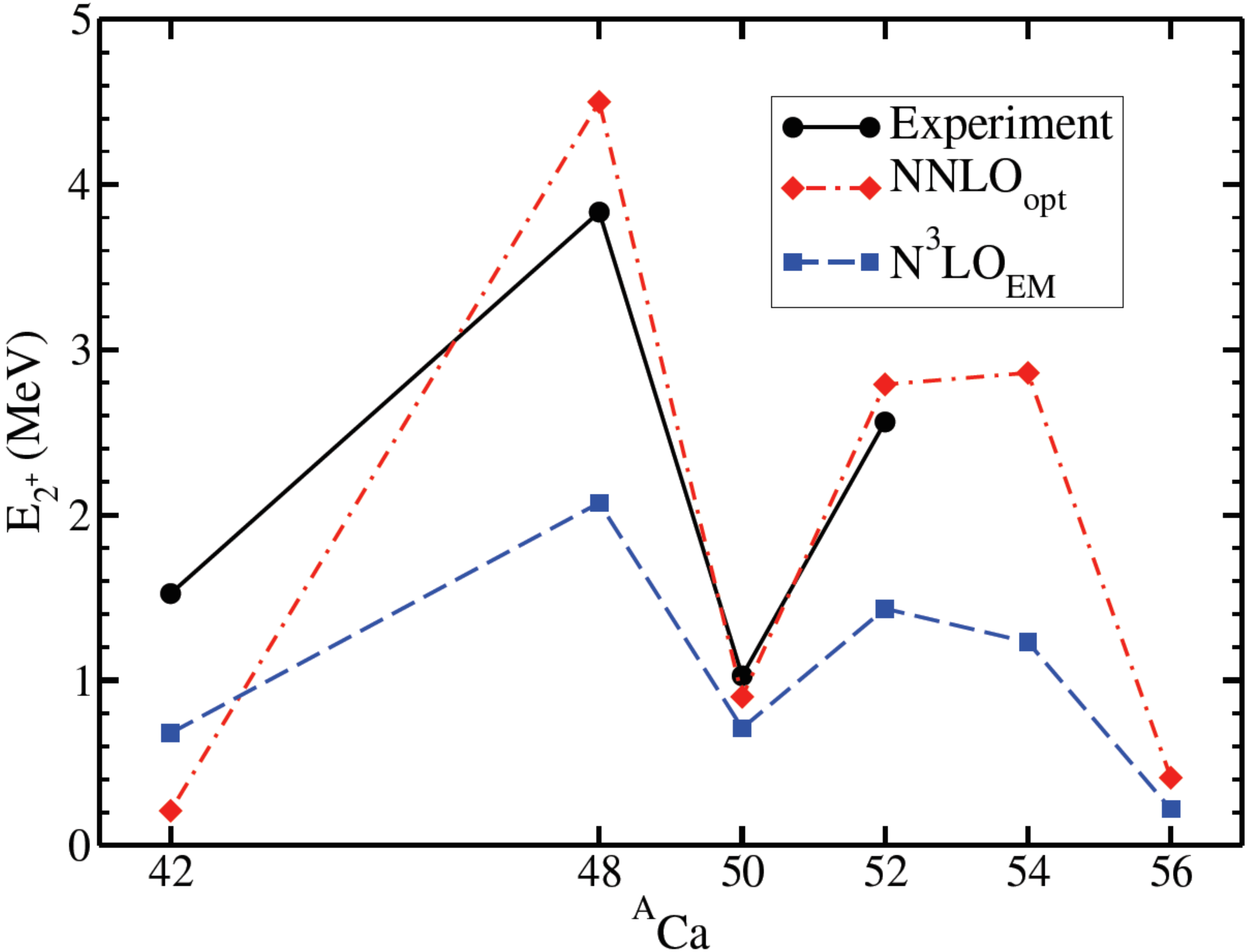

Three nucleon force

TABLE IV. Ground-state energies (in MeV) and point proton radii (in fm) for ^{3}H, ^{3}He, and ^{4}He using the NNLO$_{\mathrm{opt}}$ with and without the NNLO 3NF interaction for $c_D = -0.20$ and $c_E = -0.36$.

	$E(^3\mathrm{H})$	$E(^3\mathrm{He})$	$E(^4\mathrm{He})$	$r_p(^4\mathrm{He})$
NNLO	-8.249	-7.501	-27.759	1.43(8)
NNLO+NNN	-8.469	-7.722	-28.417	1.43(8)
Experiment	-8.482	-7.717	-28.296	1.467(13)

Three-nucleon forces

- Matrix elements of 3NFs up to energies E_{3max} = 14 ħω
- Insufficient to reach converged results for binding energies
- Convergence of energy differences somewhat better
- Error estimates based on variation 16 MeV ≤ ħω ≤ 22 MeV

First 2+ state	^{22}O	^{24}O	^{48}Ca
NN +3NF	2.3(3) MeV	3.5(5) MeV	4.8(7) MeV
NN only	2.5 MeV	5.0 MeV	4.5 MeV
Experiment	3.2 MeV	4.7 MeV	3.8 MeV

Neutron matter with optimized chiral interactions at NNLO

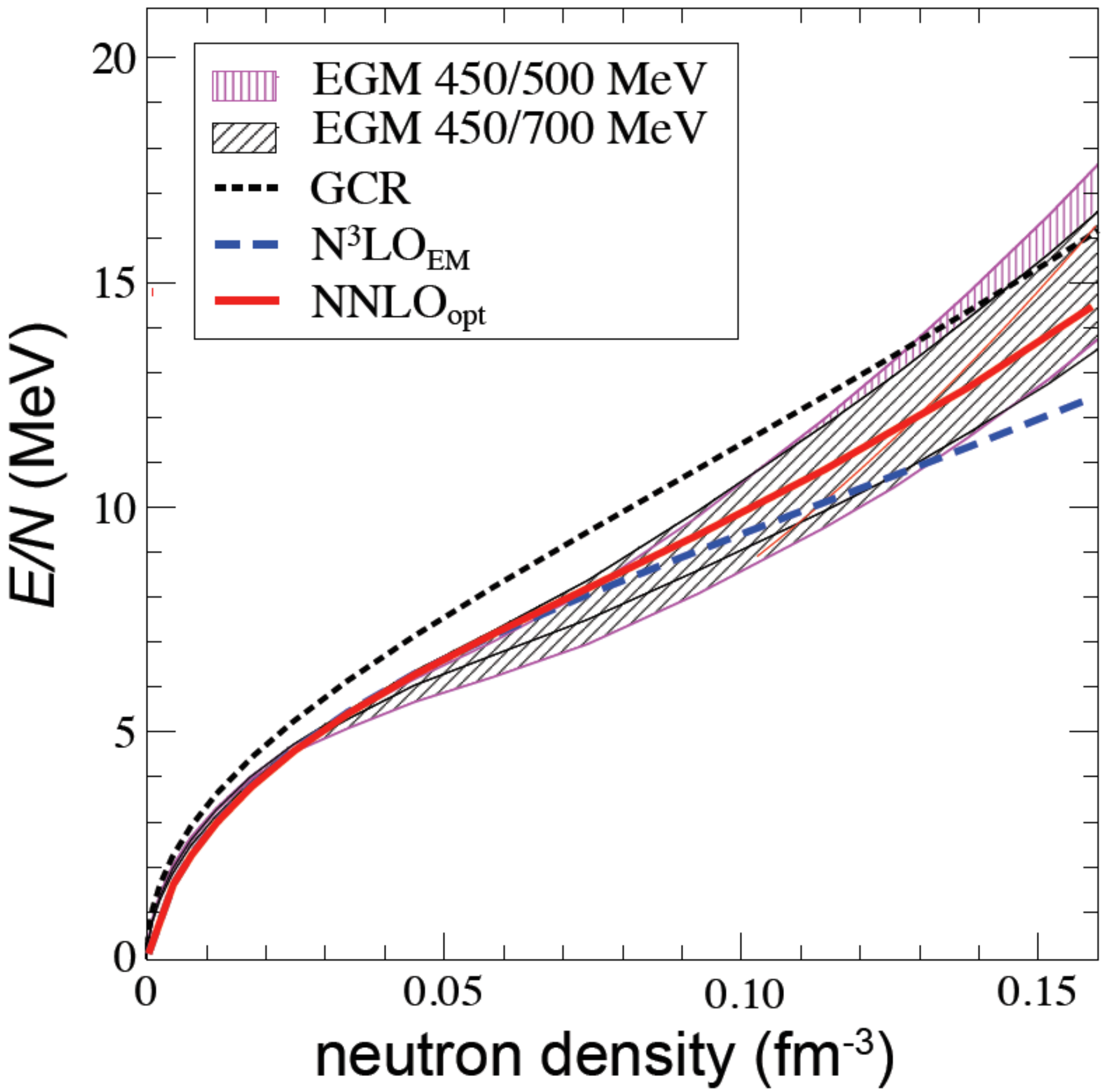

GCR=Gandolfi, Carlson, Reddy, Phys. Rev. C 85, 032801 (2012)

EGM=I. Tews, T. Krüger, K. Hebeler, and A. Schwenk, Phys. Rev. Lett. 110, 032504 (2013)

Pauli-operator from [Suzuki et al. (2000)]; Coupled cluster (and Bruckner HF)

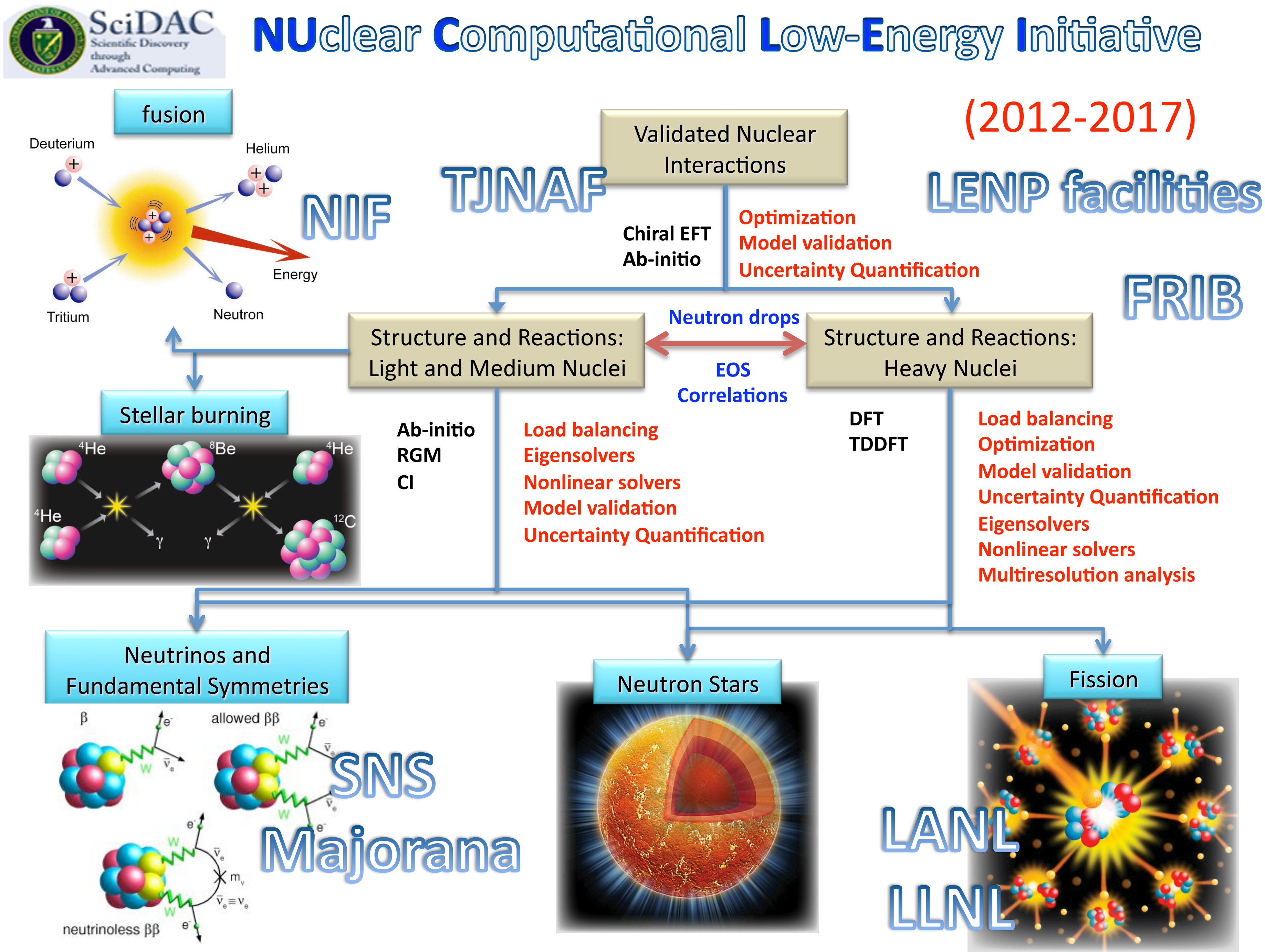

SciDAC
Scientific Discovery through Advanced Computing
NUclear Computational Low-Energy Initiative
(2012-2017)
fusion
Deuterium
Helium
Energy
Tritium
Neutron
NIF
TJNAF
Validated Nuclear Interactions
LENP facilities
FRIB
Chiral EFT
Ab-initio
Optimization
Model validation
Uncertainty Quantification
Neutron drops
Structure and Reactions: Light and Medium Nuclei
Structure and Reactions: Heavy Nuclei
EOS
Correlations
Stellar burning
^{4}He
^{8}Be
^{4}He
^{4}He
^{12}C
γ
γ
Ab-initio
RGM
CI
Load balancing
Eigensolvers
Nonlinear solvers
Model validation
Uncertainty Quantification
DFT
TDDFT
Load balancing
Optimization
Model validation
Uncertainty Quantification
Eigensolvers
Nonlinear solvers
Multiresolution analysis
Neutrinos and Fundamental Symmetries
β
allowed ββ
neutrinoless ββ
SNS
Majorana
Neutron Stars
Fission
LANL
LLNL

Summary

- Optimized functionals from UNEDF collaboration with emphasis on correlations and quantification of uncertainties

- Shell evolution in isotopes of calcium; interesting commonalities between energy functional studies and coupled-cluster method (quenching of single-particle orbitals beyond ^{60}Ca)

- Optimization of chiral interaction at NNLO